CHAPTER -4

RESULTS

RESULTS

4.1. Seasonal variations of CO_2 concentration at different heights and CO_2 flux above the canopy:

4.1.1. Variations of CO_2 concentration at different heights (µmol mol^{-1}):

4.1.1.1. Diurnal variation (monthly mean) of CO_2 concentration at eight different heights of the tower:

Results of CO_2 concentration are presented in figure 4.1.1 to 4.1.3.

4.1.1.1.1. CO_2 concentration at 2 metre (m):

Diurnal peaks of CO_2 concentration (monthly average) recorded in the month of February and March were 621 µmol mol^{-1} and 611.72 µmol mol^{-1} respectively during the early morning hours (fig 4.1.1). Minimum values of CO_2 concentration recorded in the month of February and March were 418.99 µmol mol^{-1} and 419.36 µmol mol^{-1} respectively during afternoon hours.

4.1.1.1.2. CO_2 concentration at 4 m:

At the height of 4 metre the monthly variation of CO_2 concentration are presented in fig 4.1.1. In the month of February, maximum and minimum concentrations of CO_2 were 547.91 µmol mol^{-1} and 397.89 µmol mol^{-1} respectively. In the month of March slightly higher concentration of CO_2 maximum being 555.87 µmol mol^{-1} and minimum of 402.04 µmol mol^{-1} were recorded.

4.1.1.1.3. CO_2 concentration at 6 m:

Diurnal maximum and minimum concentration (monthly average) of 495.08 µmol mol^{-1} and 398.32 µmol mol^{-1} were recorded in the month of February (fig 4.1.1). In the month of March the maximum and minimum concentrations recorded were 491.83 µmol mol^{-1} and 401.63 µmol mol^{-1} respectively (fig 4.1.1).

4.1.1.1.4. CO_2 concentration at 8 m:

During the month of February at 8 metre height maximum concentration of 475.54 µmol mol^{-1} and minimum of 399.04 µmol mol^{-1} were recorded (fig 4.1.1). The maximum and

minimum concentrations in the month of March were 482.31 µmol mol^{-1} and 402.31 µmol mol^{-1} respectively.

4.1.1.1.5. CO_2 concentration at 12 m:

Diurnal variations (monthly mean) of CO_2 concentration is represented by fig 4.1.2. In the month of February, maximum average concentration of 473.62 µmol mol^{-1} and minimum of 399.51µmol mol^{-1} were recorded. In the month of March during the morning average concentration reached a maximum of 476.55 µmol mol^{-1} whereas the average concentration decreased to 402.68 µmol mol^{-1} in afternoon around 1300 hours (fig 4.1.2).

4.1.1.1.6. CO_2 concentration at 16 m:

At the height of 16 metre, the average maximum and minimum concentration recorded in the month of February were 457.23 µmol mol^{-1} and 399.73 µmol mol^{-1} respectively (fig 4.1.2). In the month of March the maximum concentration of 460.59 µmol mol^{-1} and minimum of 402.52 µmol mol^{-1} were recorded (fig 4.1.2).

4.1.1.1.7. CO_2 concentration at 20 m:

The average canopy height of the forest during the period of measurement was 20 metre. At this height, the monthly maximum CO_2 concentration (diurnal average) of 448.95 µmol mol^{-1} and 457.47 µmol mol^{-1} were recorded in February and March respectively (fig 4.1.2). The minimum concentration observed in February and March were 399.73 µmol mol^{-1} and 403.19 µmol mol^{-1} respectively.

4.1.1.1.8. CO_2 concentration at 37 m:

In the month of February, maximum and minimum concentrations of CO_2 were 443.53 µmol mol^{-1} and 400.33 µmol mol^{-1} respectively (fig 4.1.2). Maximum and minimum half hourly average CO_2 concentration recorded in the month of March were 454.06 µmol mol^{-1} and 403.50 µmol mol^{-1} respectively (fig 4.1.2).

4.1.1.2. CO_2 concentration measured by the EC system:

The concentrations of CO_2 were also being measured above the canopy (37 metre) at frequency of 10 Hz with the help of CO_2-H_2O enclosed path analyzer (LI 7200). The average concentrations of CO_2 for each month are represented by figure 4.1.3. Results of

complete one year cycle from January 2016 to February 2017 are presented here. Peak CO_2 concentration (monthly average) of 403.62 µmol mol^{-1} was recorded in the month of June 2016, whereas lower CO_2 concentration of 380.16 µmol mol^{-1} was recorded in the month of April. The CO_2 concentration decreased gradually from February (401.68 µmol mol^{-1}) to April (380.16 µmol mol^{-1}). After that the concentration started to increase and attained a high peak of 403.62 µmol mol^{-1} in June, 2016. It again decreased up to 390.99 µmol mol^{-1} in August. The average concentration increased slightly and reached 394.13 µmol mol^{-1} in the month of September. After that the CO_2 concentrations were 389.34 µmol mol^{-1} and 382.09 µmol mol^{-1} in October and November respectively. The concentration attained a high value of 401.70 µmol mol^{-1} in the month of December and decreased thereafter to 394.59 µmol mol^{-1} in January, 2017.

4.1.2. Variation of CO_2 flux (µmol m^{-2} sec^{-1}):

Results of diurnal variation of turbulent CO_2 flux above the canopy are presented below (figure 4.1.4):

4.1.2.1. Variation of CO_2 flux in the month of February, 2016:

The value of CO_2 flux at the beginning of the averaging period at 0000 hours was 3.03 µmol m^{-2} sec^{-1}. It started to decrease from the early morning hours and attained maximum negative value of -3.69 µmol m^{-2} sec^{-1} around 1430 hours. After that, the value of CO_2 flux increased again and attained maximum of 3.16 µmol m^{-2} sec^{-1} around 2330 hours.

4.1.2.2. Variation of CO_2 flux in the month of March:

In the month of March, maximum positive flux of 5.21 µmol m^{-2} sec^{-1} was observed at 1830 hours and minimum negative flux of -4.99 µmol m^{-2} sec^{-1} was noted before noon at 1030 hours.

4.1.2.3. Variation of CO_2 flux in the month of April:

In April, positive flux increased up to a maximum value of 7.74 µmol m^{-2} sec^{-1} around 2100 hours. The minimum flux value of -7.83 µmol m^{-2} sec^{-1} was recorded around 1330 hours.

4.1.2.4. Variation of CO_2 flux in the month of May:

The maximum and minimum value of CO_2 flux recorded in the month of May, 2016 were 7.42 µmol m^{-2} sec^{-1} (at 0030 hours) and -9.16 µmol m^{-2} sec^{-1} (at 1200 hours) respectively.

4.1.2.5. Variation of CO_2 flux in the month of June:

Initially, at the beginning of the averaging period the value of CO_2 flux was 5.91 µmol m^{-2} sec^{-1}. The monthly averaged diurnal cycle attained peak positive value of 6.16 µmol m^{-2} sec^{-1} at 0230 hours and showed minimum value of -9.97 µmol m^{-2} sec^{-1} at 1230 hours.

4.1.2.6. Variation of CO_2 flux in the month of July:

The diurnal variation (monthly mean) of CO_2 flux attained a peak of 4.59 µmol m^{-2} sec^{-1} at around 0230 hours. The minimum value of -7.42 µmol m^{-2} sec^{-1} was noted at 1230 hours.

4.1.2.7. Variation of CO_2 flux in the month of August:

The values of CO_2 flux recorded at the starting and ending of the averaging period were 4.94 µmol m^{-2} sec^{-1} and 4.69 µmol m^{-2} sec^{-1} respectively. Maximum and minimum values of 5.10 µmol m^{-2} sec^{-1} and -6.10 µmol m^{-2} sec^{-1} were observed at 2030 hours and 1130 hours respectively.

4.1.2.8. Variation of CO_2 flux in the month of September:

In the month of September, maximum CO_2 flux of 4.45 µmol m^{-2} sec^{-1} was recorded at 1830 hours. Minimum flux value of -7.68 µmol m^{-2} sec^{-1} was observed at 1130 hours.

4.1.2.9. Variation of CO_2 flux in the month of October:

Positive flux of the magnitude of 3.03 µmol m^{-2} sec^{-1} was recorded at the beginning of the averaging period. The values of recoded maxima and minima were 3.88 µmol m^{-2} sec^{-1} and -8.01 µmol m^{-2} sec^{-1}. The maximum flux value was noted at 0530 hours and minimum was at 1300 hours.

4.1.2.10. Variation of CO_2 flux in the month of November:

The diurnal average of CO_2 flux ranged between -8.06 µmol m^{-2} sec^{-1} and 2.35 µmol m^{-2} sec^{-1}. Minimum value was noted at 1230 hours and maximum at 0200 hours.

4.1.2.11. Variation of CO_2 flux in the month of December, 2016:

The diurnal cycle of average CO_2 flux started with a value of 0.63 µmol m^{-2} sec^{-1} and ended at 0.44 µmol m^{-2} sec^{-1}. Maximum and minimum value of 0.62 µmol m^{-2} sec^{-1} and -5.69 µmol m^{-2} sec^{-1} was observed at 2200 hours and 1300 hours respectively.

4.1.2.12. Variation of CO_2 flux in the month of January, 2017:

At the beginning of the averaging period (0000 hours), the diurnal average value recorded was 0.87 µmol m^{-2} sec^{-1}. It attained a peak of 1.65 µmol m^{-2} sec^{-1} at 2030 hours and minimum of -3.86 µmol m^{-2} sec^{-1} was noted at 1230 hours. Towards the end of the averaging period (2330 hours) flux value of 0.98 µmol m^{-2} sec^{-1} was recorded.

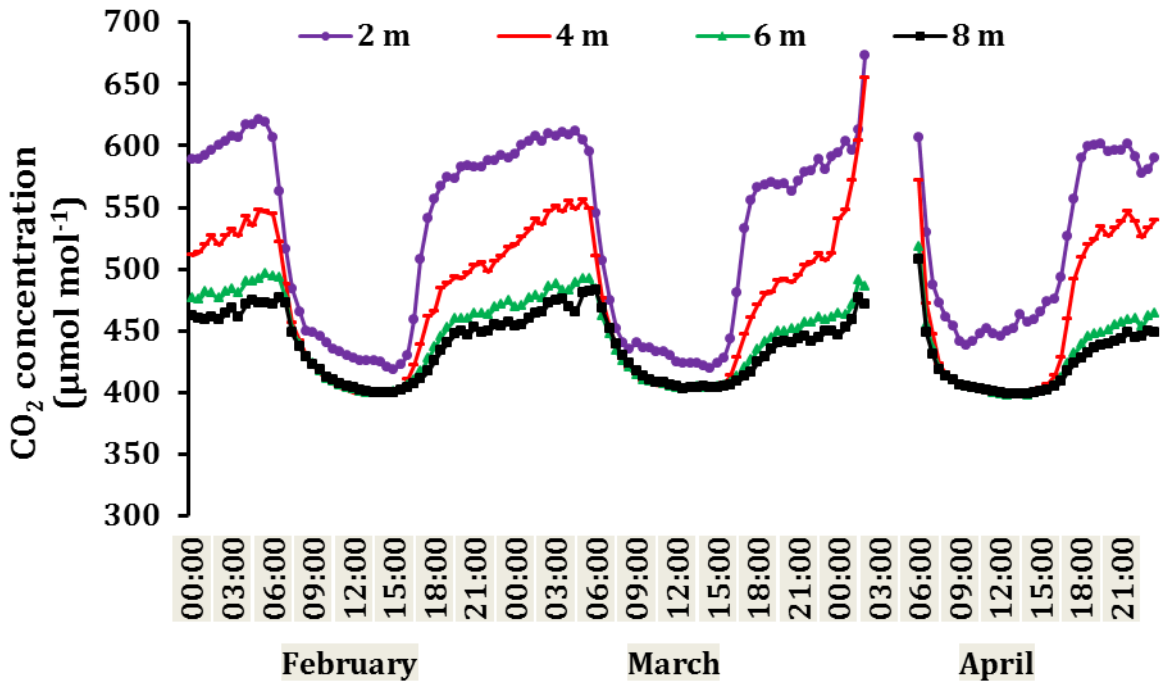

Figure 4.1.1: Diurnal variations of CO_2 concentration (monthly mean) at 2 m, 4m, 6m and 8m height.

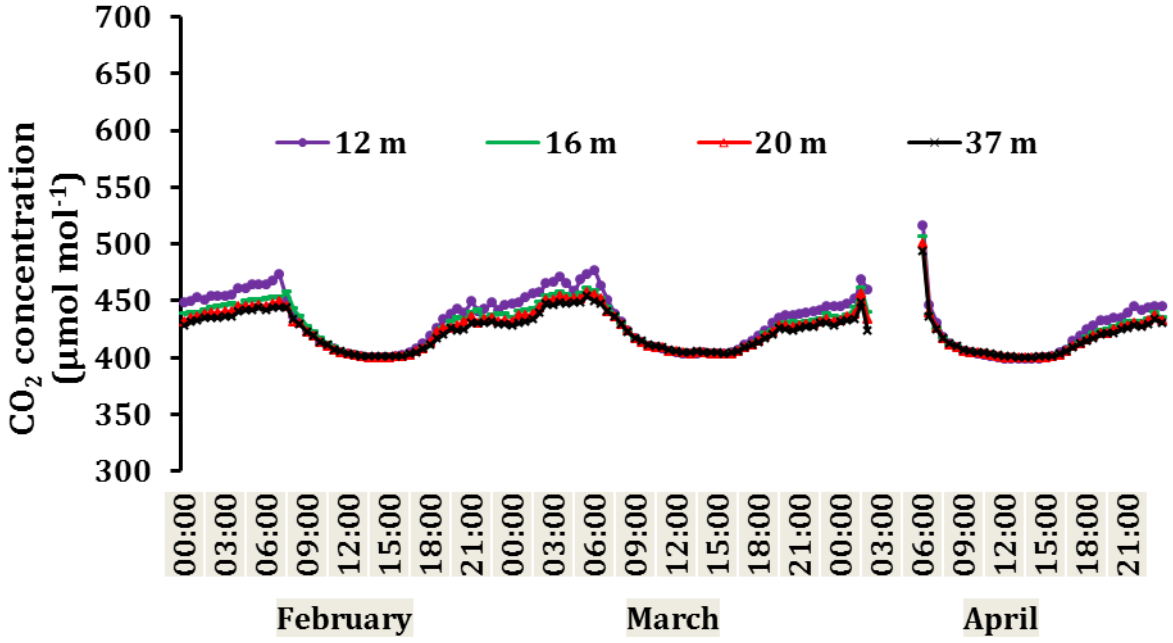

Figure 4.1.2: Diurnal variations of CO_2 concentration (monthly mean) at 12 m, 16 m, 20 m and 37 m height.

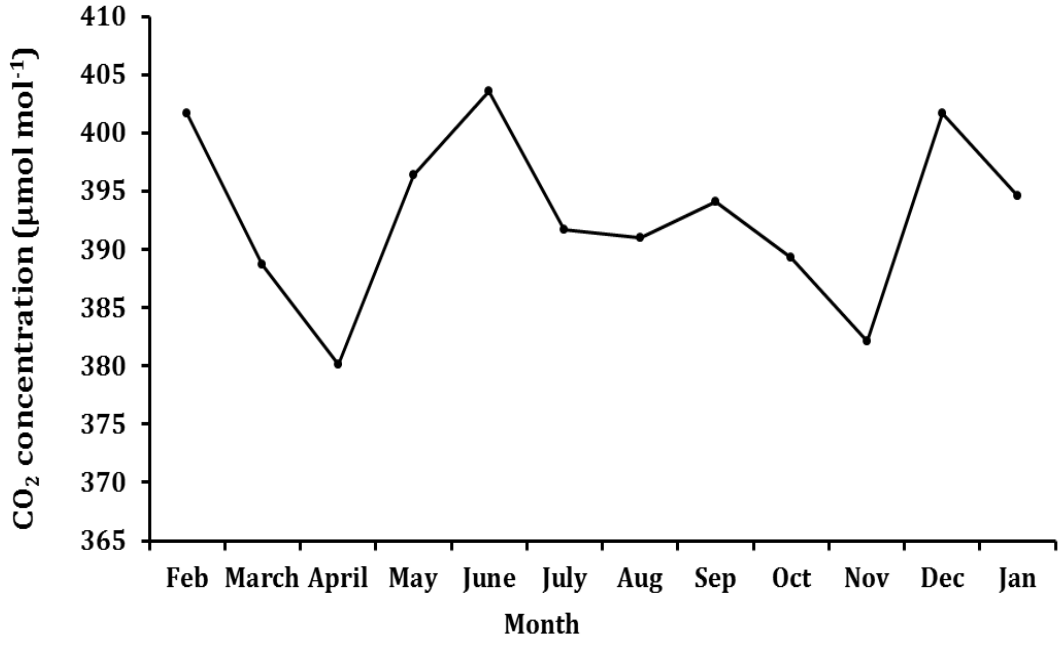

Figure 4.1.3: Monthly average CO_2 concentration measured by using CO_2-H_2O enclosed path analyzer (LI-7200).

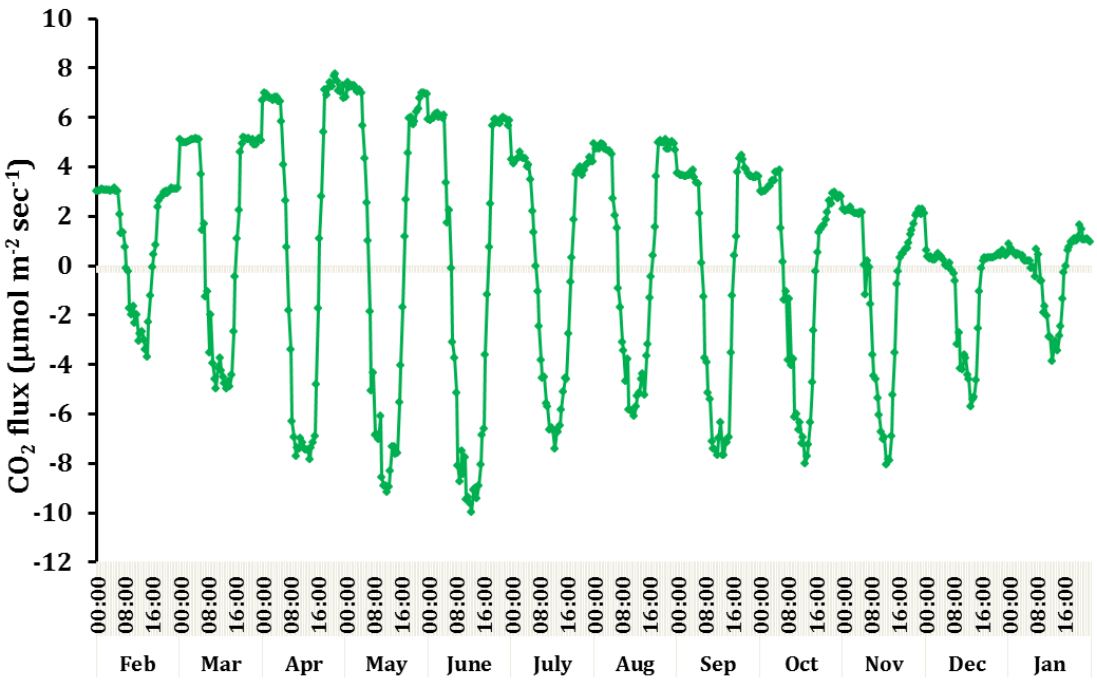

Figure 4.1.4: Monthly mean diurnal variations of half hourly CO_2 flux from February, 2016 to January, 2017.

4.2 Seasonal variations of different meteorological and plant parameters of the forest and their relationship with CO_2 flux and CO_2 concentration:

4.2.1. Variation of meteorological parameters:

4.2.1.1. Air temperature (°C):

Diurnal variations (monthly mean) of air temperature recorded inside the forest are presented in fig 4.2.1 a. During the complete annual cycle of observation maximum mean temperature of 32.10 °C was observed in the month of August at 1600 hours. Minimum temperature of 13.61 °C was recorded in the month of January, 2017 at 0630 hours. Monthly average of air temperature indicated August month to be the warmest month and January as the coldest month.

4.2.1.2. Relative humidity (%):

Diurnal variations of relative humidity (RH) has been presented by the monthly continuous plot in figure 4.2.1 b. During the whole period of measurement, half hourly average values showed maximum humidity of 89.55 % in the month of October in early morning (at 0600 hours). Lowest humidity of 40.59 % was recorded in the month of January, 2017 (at 1500 hours).

4.2.1.3. Wind speed (m s^{-1}):

Inside the forest above the canopy the measured wind speed was in the range 0.5 m s^{-1} to 4.2 m s^{-1} (fig 4.2.1 c). Wind speed gradually increased from February and attained high values in the month of April and decreased thereafter. Wind speed was very low in the month of January compared to other months.

4.2.1.4. Rain fall (mm):

The total monthly rainfall received by the site during the period of observation are depicted in figure 4.2.1 d. The annual total rainfall received by the site during the cycle of measurement was 1883.84 mm. The amount of rainfall increased from the month of February and became high 384.33 mm in April. During the monsoon season total amount of rainfall received by the site was 1032.73 mm. The rainfall received by the site was almost negligible from the month of November, 2016 to January, 2017.

4.2.1.5. Soil temperature (°C):

Soil temperature followed a similar pattern as air temperature. Diurnal variations (monthly mean) of soil temperature at 5 cm depth are presented in figure 4.2.2. Average soil temperature varied between 14.37 °C and 30.29 °C. Highest average temperature was recorded in the month of August, 2016 and minimum average temperature in the month of January, 2017.

4.2.1.6. Incoming shortwave radiation (W m^{-2}):

Diurnal variations (monthly mean) of incoming shortwave radiation are represented by figure 4.2.3. During the complete one year cycle of study highest radiation was received by the site during the mid-day period. In the month of August diurnal peak of 754.22 W m^{-2} was recorded which was the highest compared to other months. The observed monthly diurnal peak was lowest (589.5 W m^{-2}) in the month of July.

4.2.1.7. Net radiation (W m^{-2}):

The diurnal variations of net radiation are shown in figure 4.2.4. Irrespective of the months, net radiation was negative at night times. Net radiation started to attain positive values between 0500 hours to 0630 hours. Diurnal peaks of net radiation continuously increased from February to June. The diurnal peak decreased in the month of July by some amount before attaining a peak of 639.68 W m^{-2} in the month of August. The diurnal peaks were very close to each other in September and October and started to decrease slowly thereafter.

4.2.1.8. Photosynthetically active radiation (PAR):

Diurnal variations (monthly mean) of PAR are represented by figure 4.2.4. During the night and early morning hours the recorded PAR was very close to zero or negative. The pattern of diurnal variation of PAR and net radiation was almost similar. For each month diurnal peaks were recorded around noon. Diurnal peaks gradually increased from February to June and suddenly decreased in the month of July. During the whole period of measurement maximum PAR of 1542 µmol m^{-2} s^{-1} was recorded in the month of August in noon hours. After that PAR started to decline.

4.2.2. Leaf area index (LAI):

The results of calculated LAI for each month are shown in table 4.2.1. The measured LAI in January, 2016 was 0.79. LAI increased to 1.25 in the month of February. It (LAI) started to increase from March onward and recorded 2.19 in March and 2.66 in April. Highest LAI of 3.07 was recorded in the month of June. Beyond June LAI started to decline and the LAI values of August, September and October were 2.37, 2.23 and 1.85 respectively.

4.2.3. Vapour pressure deficit (VPD) (Kpa):

Diurnal variation (monthly mean) of vapour pressure deficit during the monsoon months (June, July, August and September) are depicted in figure 4.2.5. VPD values were small during the night and early morning and attained maximum during late afternoon hours. In comparison to other monsoon months, VPD values were very high in the month of August. Diurnal peak of 2.12 Kpa was recorded in the month of August around 1430 hours. Out of the whole monsoon season, the recorded day time VPD were very low in July month. Diurnal peaks recorded in the month of June and September was 1.82 Kpa and 1.77 Kpa respectively during late afternoon hours.

4.2.4. Turbulence characteristics of the site:

To interpret the turbulence characteristics of the site during different times of the day and in different seasons the following parameters were worked out.

4.2.4.1. Friction velocity (u*):

In fig 4.2.6 a, the percentage of occurrence of u* in different seasons has been stratified in four bin limits viz., 0-0.2 m s^{-1}, 0.2-0.4 m s^{-1}, 0.4-0.8 ms^{-1} and above 0.8 m s^{-1}. Occurrence percentage of u* was very high in the lower turbulence range 0-0.2 m s^{-1}. The percentage of occurrence of u* in the range 0-0.2 m s^{-1} during winter and post monsoon season were approximately 65%. In the pre-monsoon season the percentage of occurrence of u* in the bin widths 0.2-0.4 m s^{-1}, 0.4-0.8 m s^{-1} and above 0.8 m s^{-1} were 26.53 %, 31.03 % and 7.88 % respectively. During the monsoon season recorded occurrence percentage of u* in the bin limits 0.2-0.4 m s^{-1}, 0.4-0.8 m s^{-1} and above 0.8 m s^{-1} were 29.41%, 20.71% and 1.04 % respectively.

Variation of u*(separately in day and night) in the above bin limits has been analysed and presented in fig 4.2.6 (c-d). Occurrence percentage of u* during day time in bin limits 0.2-0.4 ms^{-1} and 0.4-0.8 ms^{-1} in the whole period of study were 36.18 % and 41.46 % respectively. During night-time occurrence percentages of u* was very high in the range 0-0.2 m s^{-1}. In winter and post monsoon nights the occurrence percentage of u* in lower turbulence range (0-0.2 m s^{-1}) were 92 % and 93 % respectively. During night time in the pre-monsoon season the occurrence percentages of u* in the bin limits 0.2-0.4 m s^{-1}, 0.4-0.8 m s^{-1} and above 0.8 m s^{-1} were 25.92, 16.36 and 3.78 % respectively.

4.2.4.2. Standard deviation of vertical velocity (σ_w):

To interpret the turbulence characteristics of the site, the turbulence parameter σ_w has been stratified in to five different class viz., 0-0.2 m s^{-1}, 0.2-0.4 m s^{-1}, 0.4-0.8 m s^{-1} and above 0.8 m s^{-1}(figure 4.2.6 b). During the whole period of study, occurrence of σ_w was highest (44.32 %) in the lower turbulence range 0-0.2 m s^{-1}. Lower turbulence events (0-0.2 m s^{-1}) were very high in winter and post monsoon season with occurrence percentage of around 60%. Out of three higher turbulence levels occurrence percentages of σ_w was highest in the range 0.4-0.8 m s^{-1} in all the seasons.

Seasonal as well as day-night variation of σ_w occurrence are presented in fig 4.2.6(e-f). Day time variation of σ_w (fig 4.2.6 e) showed higher percentage of occurrences in the level 0.4-0.8 m s^{-1} during all the seasons. In the bin width 0.4-0.8 m s^{-1}, the percentage of occurrences of σ_w in winter, pre-monsoon, monsoon and post monsoon seasons were 66.90, 59.20, 66.67 and 61.29% respectively.

During night time (fig 4.2.6 f) in the lower turbulence bin width (0-0.2 m s^{-1}), the occurrence percentage of σ_w in winter and post monsoon season were around 90%. During night time of pre-monsoon season the occurrence percentages of σ_w recorded in the ranges 0.2-0.4 m s^{-1}, 0.4-0.8 m s^{-1} and above 0.8 m s^{-1} were 26.77, 21.79 and 6.58% respectively.

4.2.4.3. Stability parameter (z-d/L):

In the stability parameter, '*L'* is obukhov length,'d' is zero plane displacement and 'z' is the height of measurement. Seasonal and day-night variation of atmospheric stability parameter (z-d/L) has been stratified in five different classes viz., less than -1(very unstable), -1 to -0.05(moderately unstable), -0.05 to 0.05(neutral), 0.05 to 1 (stable) and

greater than 1 (very stable). In the complete annual cycle of measurement, occurrence percentage of (z-d/L) was highest (29.85 %) in the moderately unstable range (fig 4.2.7 a).

Day time analysis (fig 4.2.7 b) showed highest occurrence percentages of (z-d/L) in the moderately unstable range irrespective of seasons. Night time analysis (fig 4.2.7 c) indicated higher occurrence percentages in stable and very stable ranges.

4.2.5. Surface heat fluxes:

4.2.5.1. Latent heat flux (W m^{-2}):

Monthly continuous diurnal variation of latent heat fluxes are shown in figure 4.2.8. The diurnal pattern of variation of latent heat flux was similar to the variation in net radiation (Rn). The half hourly averaged latent heat flux values were very small and sometimes negative during the night time. In the beginning of the measurement the monthly averaged diurnal peak of LE flux recorded in the month of February, 2016 was 191.90 W m^{-2}. After that gradual increase in diurnal peak of LE was observed and attained a value of 394.91 W m^{-2} in the month of April at 1230 hours. The diurnal peaks decreased thereafter and were almost equal in the month of May and June. It decreased further and attained a value of 286.68 W m^{-2} in the month of July at 1300 hours. The diurnal peak of LE flux suddenly increased in the month of August and attained a value of 390.32 W m^{-2} around 1130 hours. The diurnal peak decreased gradually from the month of September and attained minimum value of 135.35 W m^{-2} in the month of January, 2017.

4.2.5.2. Sensible heat flux (W m^{-2}):

Diurnal variation of sensible heat (fig 4.2.8) also followed the same pattern of diurnal variation as net radiation. Sensible heat flux values were observed to be negative during night and early morning hours. At the beginning of our measurement the diurnal peak of sensible heat was 175.97 W m^{-2}. After that it decreased slowly up to April and attained a value of 114.69 W m^{-2}. The observed diurnal peak in the month of May was 117.26 W m^{-2}. It decreased slowly after that and attained minimum of 82.67 W m^{-2} in July. From the month of August diurnal peak increased slowly and attained its maximum value of 217.71 W m^{-2} in the month of January, 2017. Exceptionally slight decrease in diurnal peak was observed in the month of October as compared to September.

4.2.5.3. Latent heat flux vs sensible heat flux:

From the energy partitioning analysis in figure 4.2.8, it is clear that latent heat flux dominated sensible heat flux during the period of study except for the month of January, 2017. The difference was very marginal in the month of February. The recorded diurnal peaks of LE and H in the month of February were 191.90 W m^{-2} and 175.97 W m^{-2} respectively. The diurnal peaks of LE and H noted in the month of January were 135.35 W m^{-2} and 217.71 W m^{-2} respectively.

4.2.5.4. Evapotranspiration (ET) (mm hr^{-1}):

Monthly continuous plot of diurnal variation of ET are shown in figure 4.2.9. Observed ET values were very small and sometimes negative during night time. Maximum evapotranspiration was observed around noon hours. At the beginning of the measurement in the month of February the diurnal peak of 0.28 mm hr^{-1} was noted around 1230 hours. It increased thereafter and attained its peak value of 0.58 mm hr^{-1} in the month of April around 1230 hours. After that, the monthly diurnal peaks decreased gradually and attained a value of 0.43 mm hr^{-1} in the month of July. It again increased in the month of August and gradually decreased thereafter until it reached the minimum of 0.19 mm hr^{-1} in the month of January. The annual average of the estimated ET was 2.8± 0.19 mm day^{-1}.

4.2.6. Energy balance closure:

Energy balance closure of the study area has been estimated with the help of net radiation (Rn), soil heat flux (G), latent heat flux (LE) and sensible heat flux (H).

4.2.6.1. Energy balance closure of the whole period:

4.2.6.1.1. Energy balance closure using half hourly data:

Energy balance closure calculated using half hourly averaged data of Rn, G, LE and H are presented in figure 4.2.10 a. The slope and intercept of the regression in the scatter plot between Rn-G and H + LE is 0.78 and 10.71 respectively (R^2=0.86). Therefore, the energy balance closure estimated using half hourly average of the data was 78 %.

4.2.6.1.2. Energy balance closure using daily averaged data:

Energy balance closure of the site has also been tested using the daily average of the parameters Rn, G, LE and H. In this case (fig 4.2.10 b), the slope and intercept of the regression is 0.85 and 1.92 respectively with R^2= 0.83. Here the recorded energy balance closure was 85 %.

4.2.6.2. Energy balance closure in different turbulence and stability conditions:

An attempt was made to analyse the impact of different atmospheric turbulence and stability conditions on energy balance closure.

4.2.6.2.1. Effect of friction velocity (u*) on energy balance:

Energy balance closure estimated on different u* classes are plotted in fig 4.2.11(a-d). The energy balance closure estimated in u* class (0-0.2 m s^{-1}) was 51%. The closure increased to 72 % in the next bin limit (0.2-0.4 m s^{-1}). At very high atmospheric turbulence conditions, in 0.4-0.8 m s^{-1} and above 0.8 m s^{-1} the estimated closure was 86 and 93% respectively.

4.2.6.2.2. Effect of standard deviation of vertical velocity (σ_w) on energy balance:

In fig 4.2.12 (a-d), energy balance closure has been tested in four different classes of σ_w. Closure was very poor (≈ 14 %) in the σ_w range 0-0.2 m s^{-1}. In the next class (0.2 m s^{-1} to 0.4 m s^{-1}) the closure increased to 59%. The closure recorded in high turbulence levels 0.4 m s^{-1} to 0.8 m s^{-1} and above 0.8 m s^{-1} were 81 and 92% respectively.

4.2.6.2.3. Effect of different stability conditions on energy balance:

Variation in energy balance closure with atmospheric stability are shown in figure 4.2.13(a-e). In very unstable condition ((z-d)/L<-1) the closure recorded was 71%. The closure increased up to 82% in moderately unstable condition, (-1< (z-d)/L< -0.05). Highest closure of ≈84 % was noted in neural conditions, (-0.05< (z-d)/L <0.05). After that the energy balance closure decreased to 46% in stable conditions, (0.05< (z-d)/L<1). Poor closure ≈14% was noted in very stable conditions of the atmosphere, (z-d)/L>1.

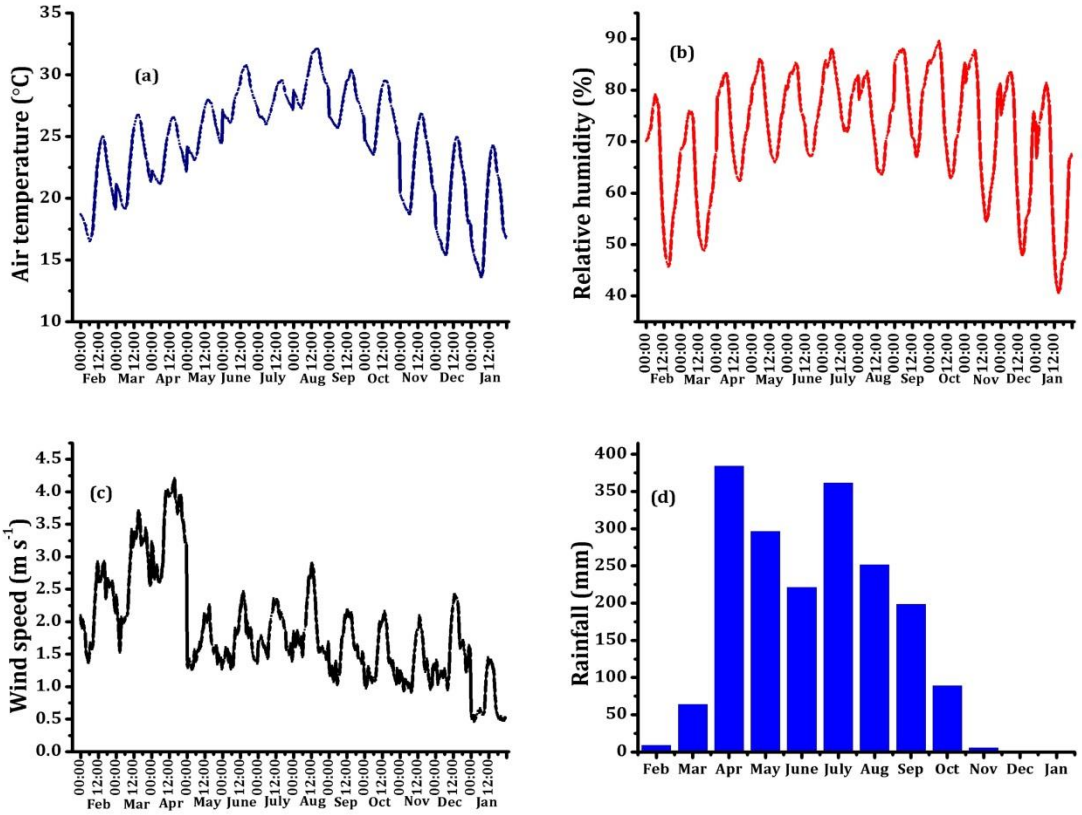

Figure 4.2.1: (a) Diurnal variations of air temperature (monthly mean) from February, 2016 to January 2017, (b) diurnal variations of relative humidity (monthly mean) from February 2016 to January 2017, (c) diurnal variations in wind speed (monthly mean) from February 2016 to January 2017 and (d) monthly total rainfall recorded in the study area from February 2016 to January 2017.

Figure 4.2.2: Diurnal variations of soil temperature (monthly mean) from February, 2016 to January, 2017.

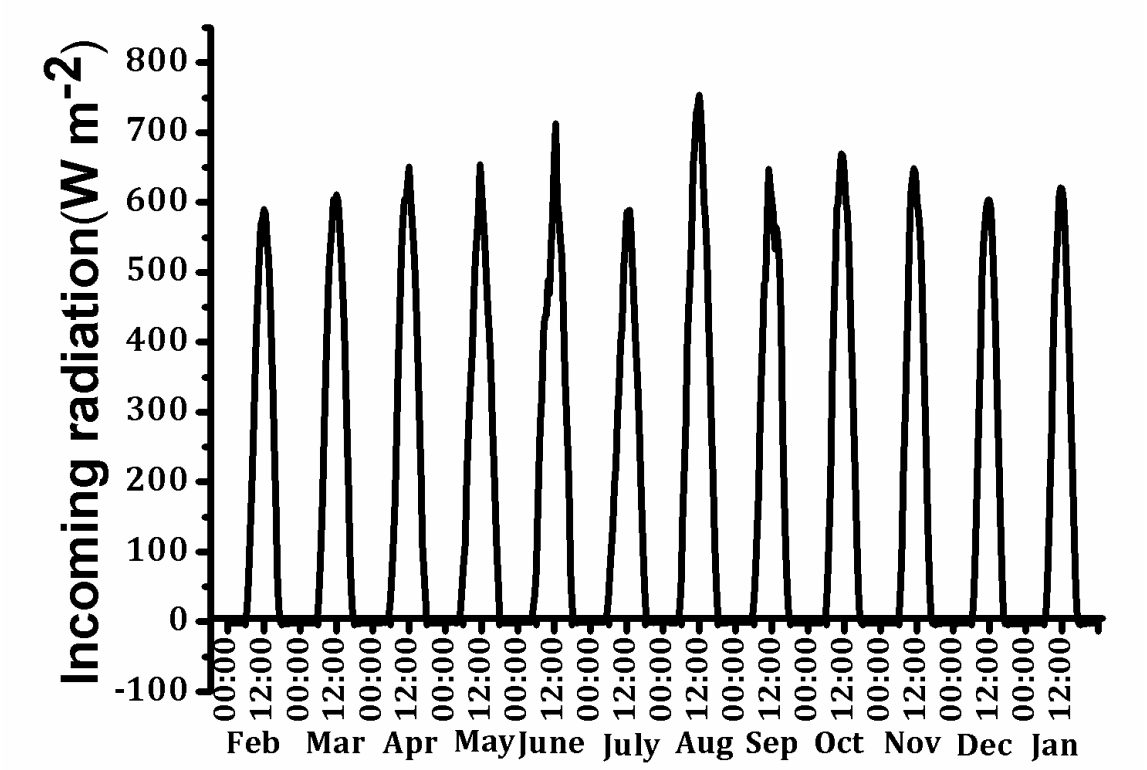

Figure 4.2.3: Diurnal variations of incoming solar radiation (monthly mean) from February, 2016 to January, 2017.

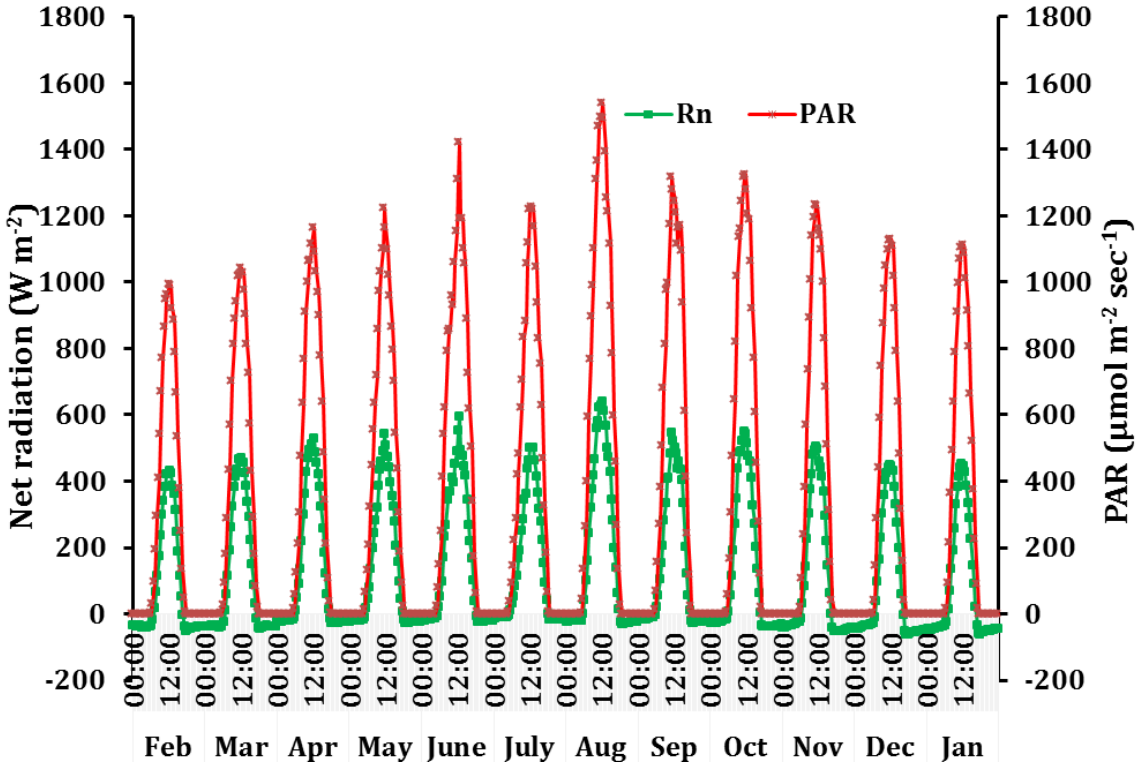

Figure 4.2.4: Diurnal variations of net radiation and photosynthetically active radiation (monthly mean) from February 2016 to January 2017.

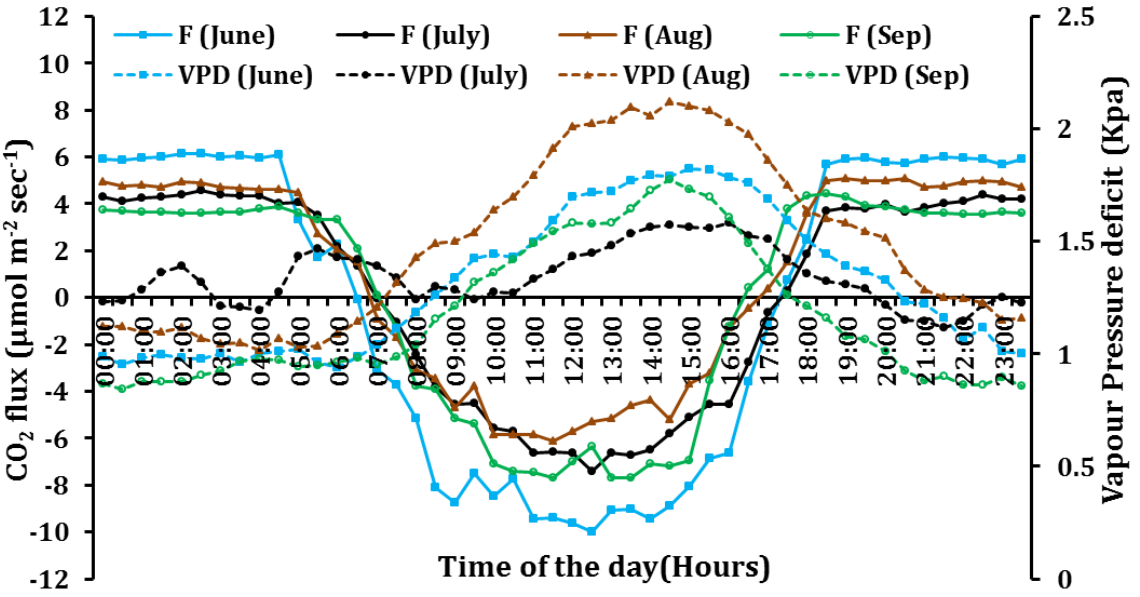

Figure 4.2.5: Diurnal variations (monthly mean) of CO_2 flux (indicated by 'F') and VPD from June 2016 to September 2016.

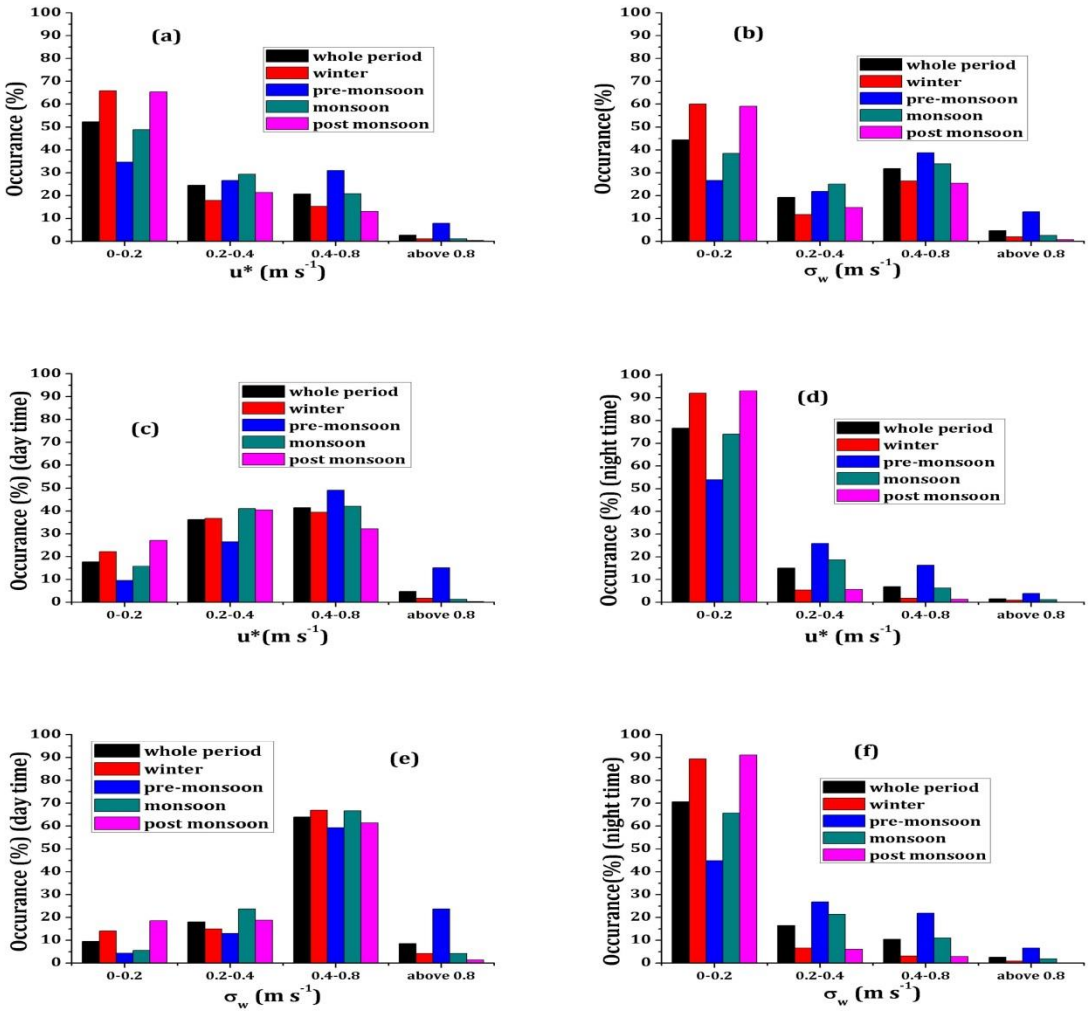

Figure 4.2.6: (a) Occurrence of friction velocity (u^*) in different bin limits during whole period and in different seasons. (b) Occurrence of standard deviations of vertical velocity fluctuations (σ_w) in different bin limits during whole period and in different seasons. (c) Occurrence of friction velocity (u^*) in different bin limits during whole period and in different seasons during day time. (d) Occurrence of friction velocity (u^*) in different bin limits during whole period and in different seasons during night time. (e) Occurrence of standard deviations of vertical velocity fluctuations (σ_w) in different bin limits during whole period and in different seasons during day time. (f) Occurrence of standard deviations of vertical velocity fluctuations (σ_w) in different bin limits during whole period and in different seasons during night time.

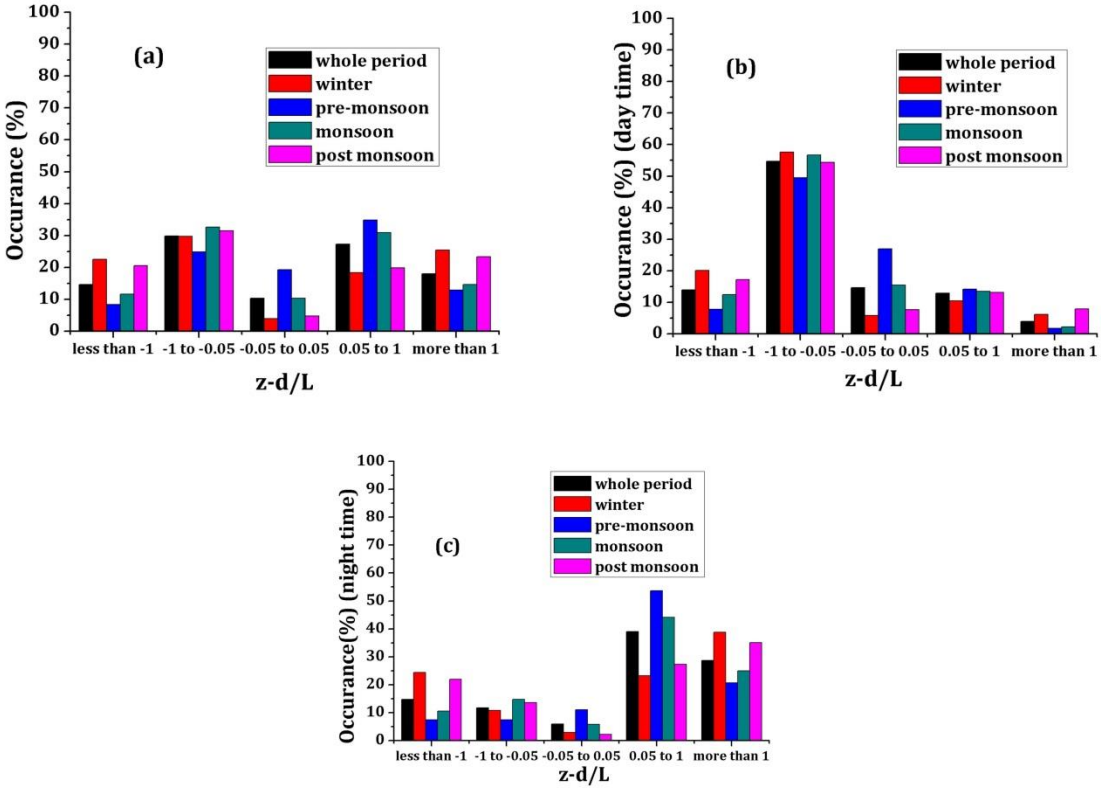

Figure 4.2.7: (a) Occurrence of stability parameter (*z-d/L*) in different bin limits during whole period and in different seasons. (b) Occurrence of stability parameter (*z-d/L*) in different bin limits during whole period and in different seasons during day time. (c) Occurrence of stability parameter (*z-d/L*) in different bin limits during whole period and in different seasons during night time.

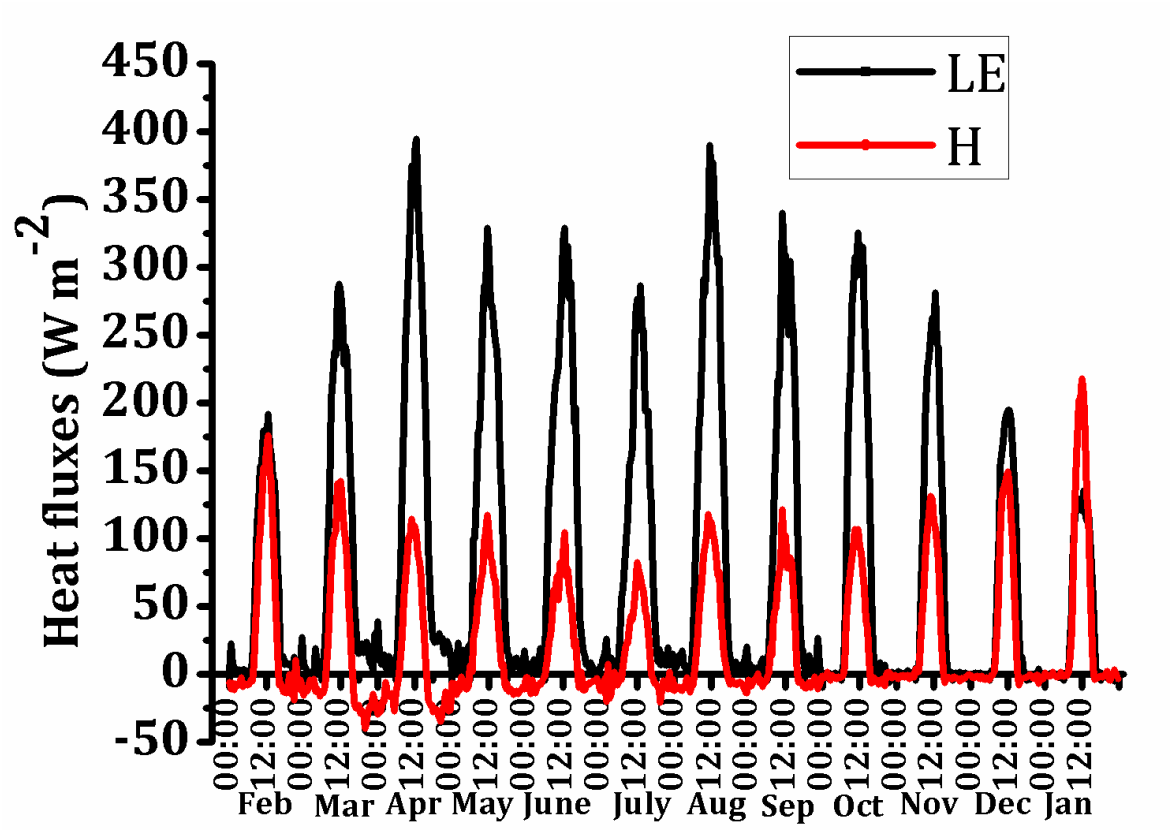

Figure 4.2.8: Diurnal variations of latent heat and sensible heat fluxes (monthly mean) from February 2016 to January 2017.

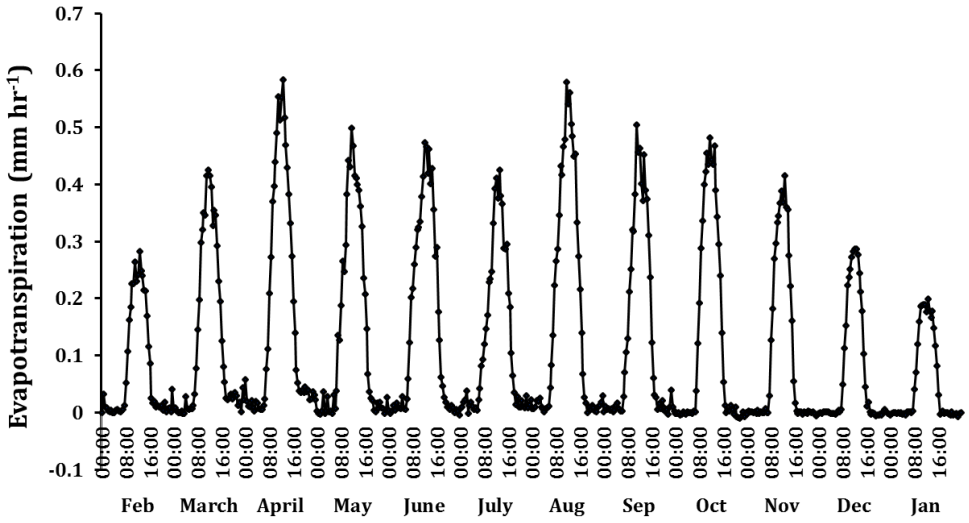

Figure 4.2.9: Diurnal variation (monthly mean) of evapotranspiration.

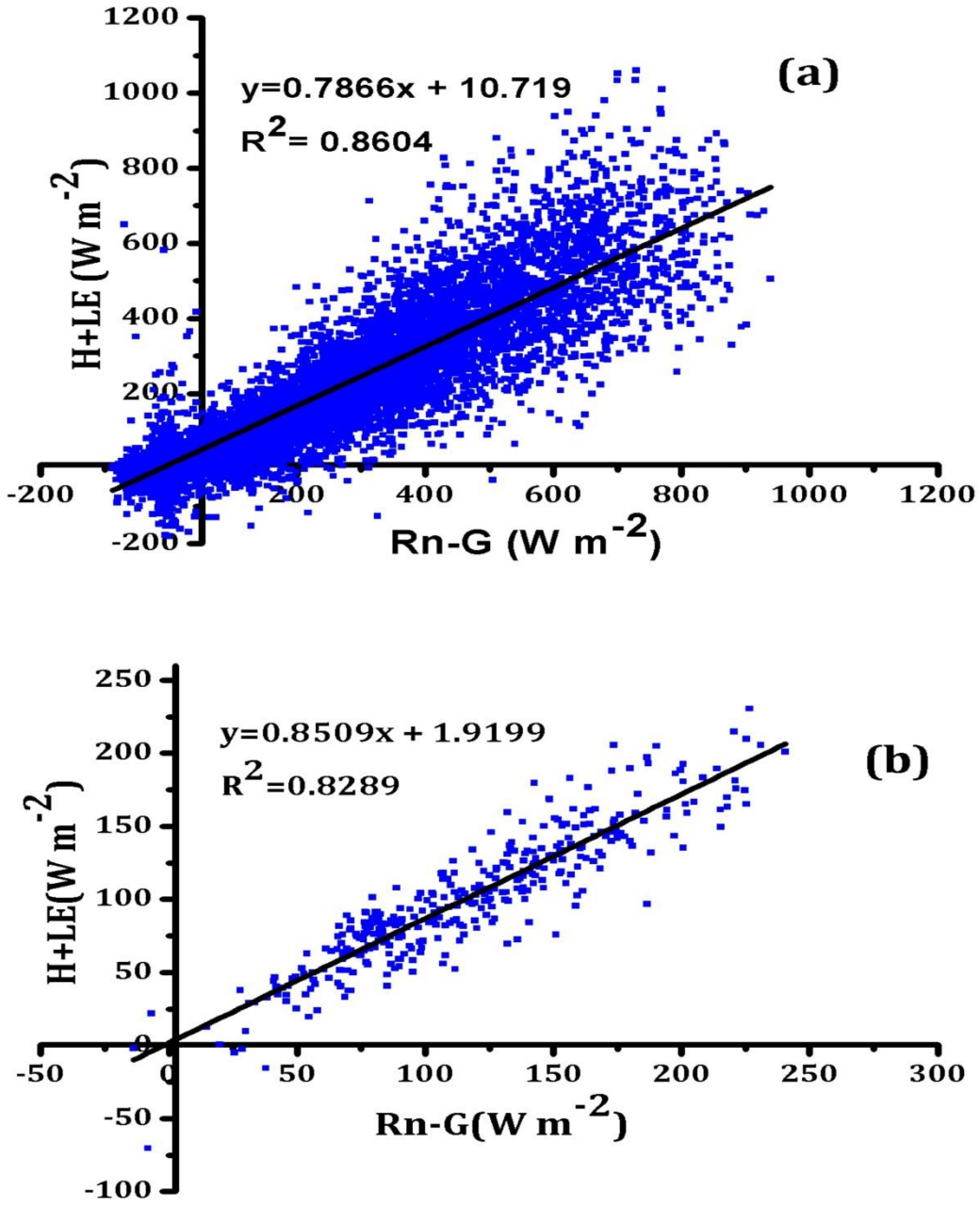

Figure 4.2.10: (a) Energy balance closure of the whole study period considering half hourly averaged data. (b) Energy balance closure of the whole study period considering daily average of data.

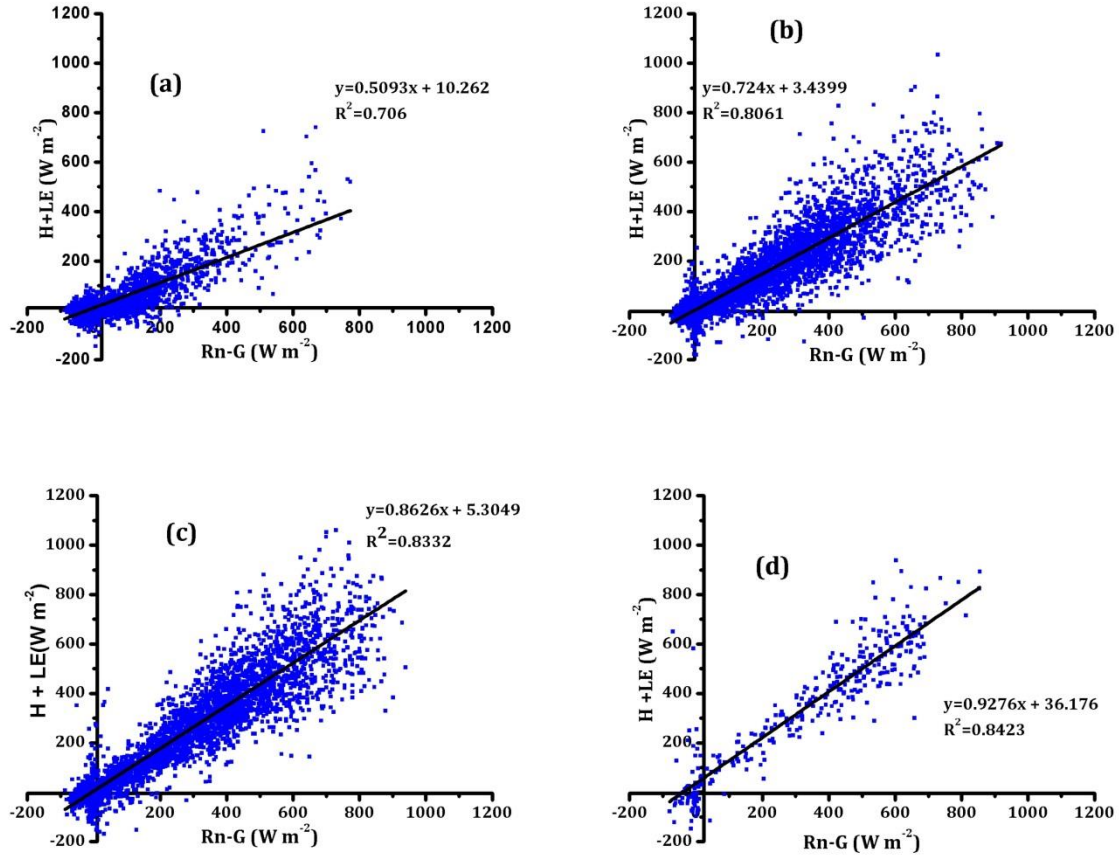

Figure 4.2.11: Energy balance closure in different friction velocity (u*) classes (a) 0 to 0.2 m s^{-1}(b) 0.2 to 0.4 m s^{-1} (c) 0.4 to 0.8 m s^{-1} (d) above 0.8 m s^{-1}.

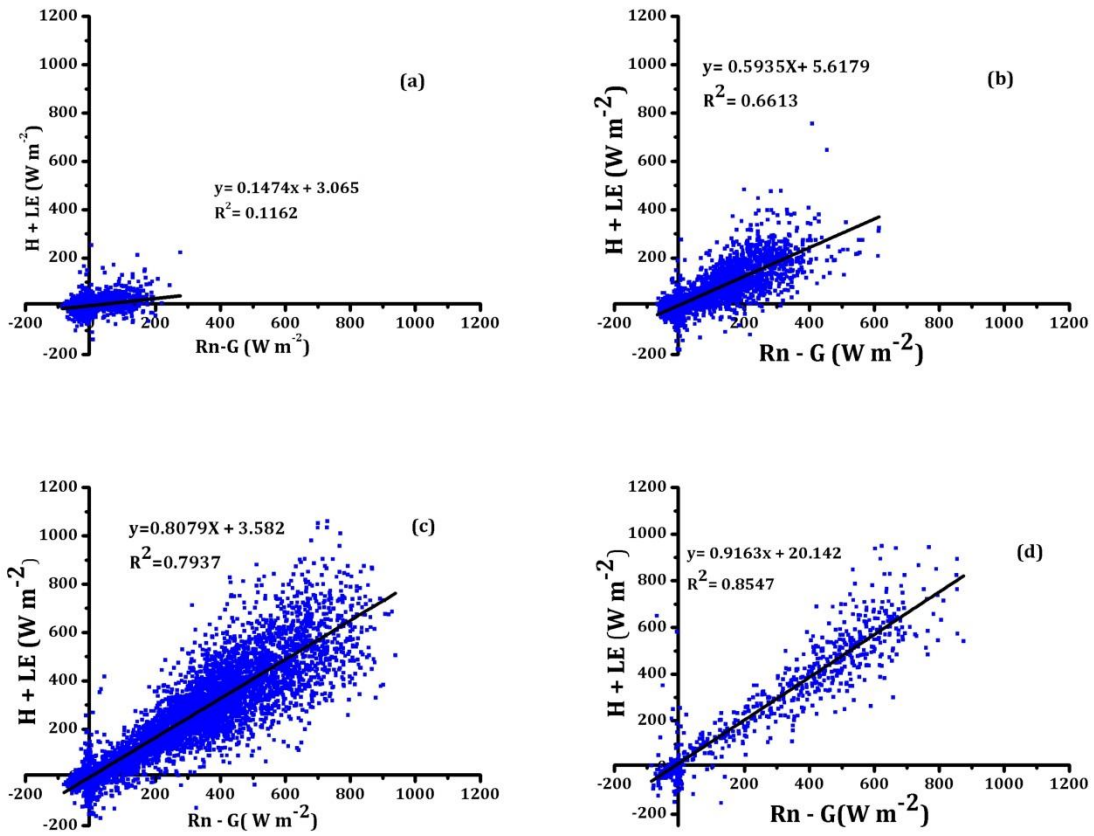

Figure 4.2.12: Energy balance closure in different classes of standard deviations of vertical velocity fluctuations (σ_w); (a) 0 to 0.2 m s^{-1},(b) 0.2 to 0.4 m s^{-1} (c) 0.4 to 0.8 m s^{-1} (d) above 0.8 m s^{-1}.

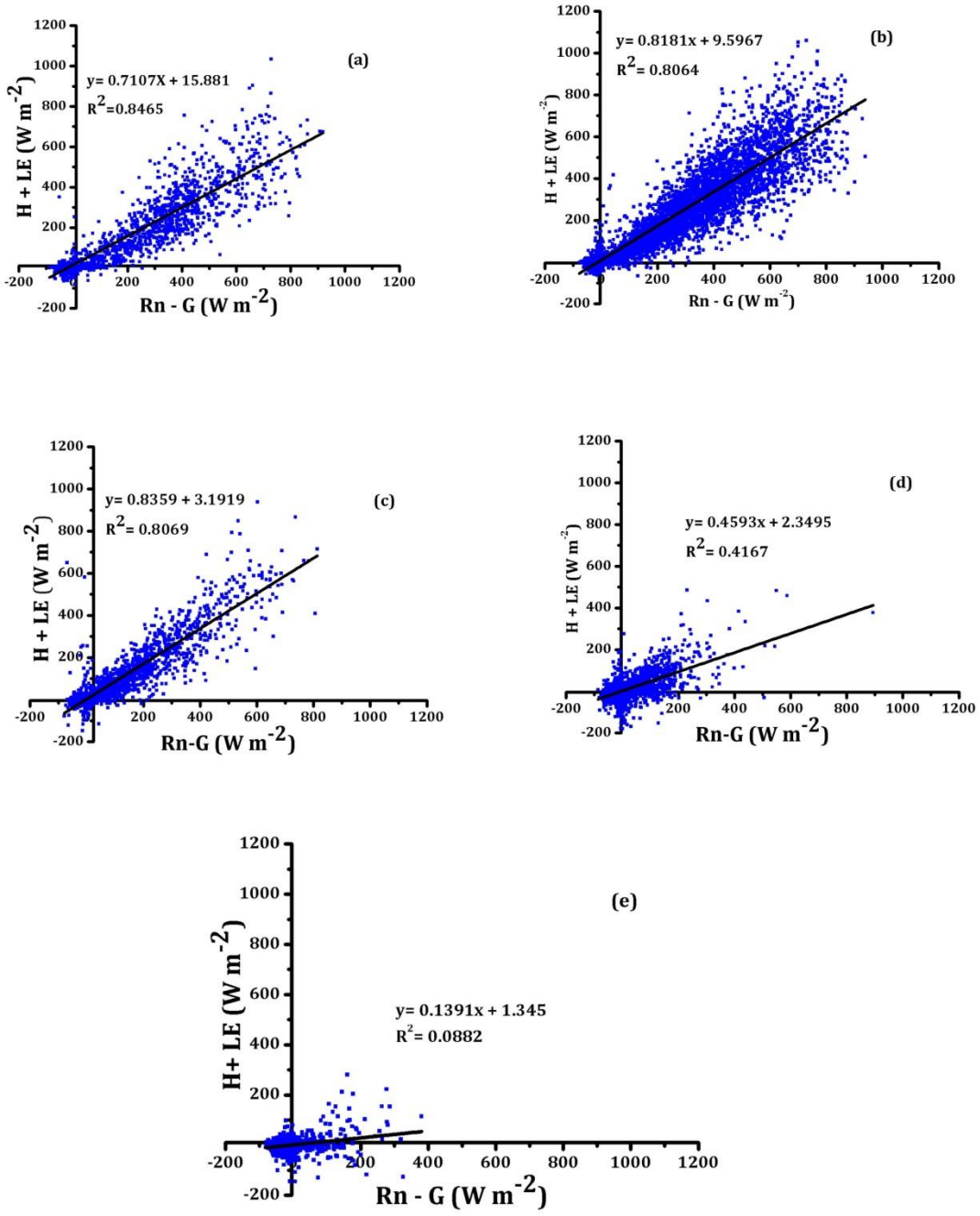

Fig 4.2.13: Energy balance closure in different stability (*z-d/L*) classes (a) less than -1 ,(b) -1 to -0.05 (c) -0.05 to 0.05 (d) 0.05 to 1 (e) greater than 1.

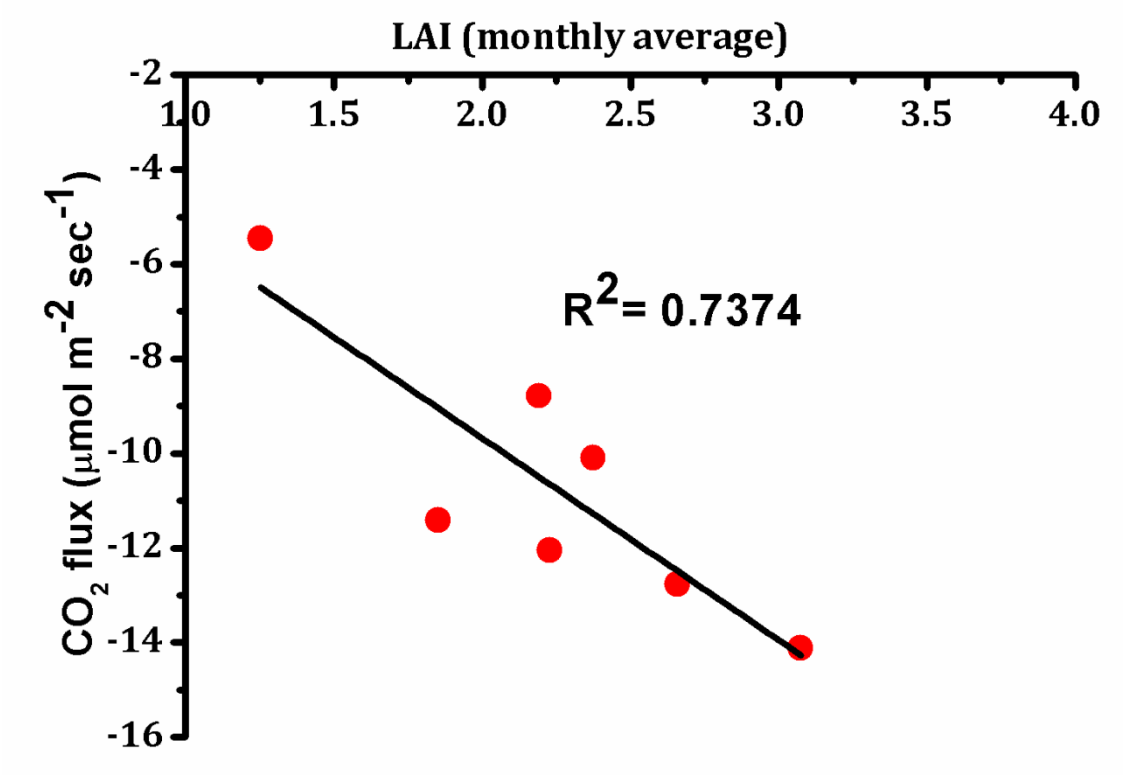

Figure 4.2.14: Relationship between monthly averaged LAI and maximum monthly value of negative CO_2 flux during the period of study.

Table 4.2.1: Monthly variation of average leaf area index (LAI) in the year 2016.

Month	**LAI**
February	1.25
March	2.19
April	2.66
June	3.07
August	2.37
September	2.23
October	1.85

4.3. Partitioning of net CO_2 flux into its components and their relationship with PAR and other meteorological parameters:

4.3.1. Partitioning of Net ecosystem exchange:

4.3.1.1. Variation in gross primary production (GPP):

Average values of daily GPP are shown in figure 4.3.1 a. The estimated (daily average) GPP of the forest ranged between 1.58 g C m^{-2} day^{-1} and 15.86 g C m^{-2} day^{-1}. The daily estimated GPP of the forest ecosystem under study gradually increased from the month of February and attained highest value of 15.86 g C m^{-2} day^{-1} in the last week of April. In the month of May and June most of observed GPP values were higher. After that, daily averaged GPP values decreased in the months of July and August. Observed daily averaged GPP values again increased slightly in the month of September and gradually decreased thereafter and attained the minimum of 1.58 g C m^{-2} day^{-1} in the first half of January, 2017. The annual GPP of the forest during our period of study (February, 2016 to January, 2017) is estimated as 2660.07 g C m^{-2} yr^{-1}.

4.3.1.2. Variation in Ecosystem respiration (g C m^{-2} day^{-1}):

Daily averages of ecosystem respiration are presented in figure 4.3.1 b. The trend of daily variation of ecosystem respiration is very similar to variation of GPP. Maximum daily respiration of 15.06 g C m^{-2} day^{-1} was estimated during the last part of May. Daily average ecosystem respiration attained minimum value of 0.06 g C m^{-2} day^{-1} in the first part of January, 2017. The estimated annual ecosystem respiration of the forest is 2567.13 g C m^{-2} yr^{-1}.

4.3.2. Variation in NEP (g C m^{-2} day^{-1}):

Daily average values of NEP are represented by figure 4.3.2 a. In the complete annual cycle studied, daily average of GPP fluctuated between -6.63 g C m^{-2} day^{-1} and 5.03 g C m^{-2} day^{-1}. On annual scale the NEP of the forest was estimated as 92.93± 1.7 g C m^{-2} yr^{-1}. The daily maximum NEP was observed during the month of May. Monthly sums of net ecosystem productivity are shown in figure 4.3.2 b. Highest monthly total NEP of 32.45 g C m^{-2} was estimated in the month of June.

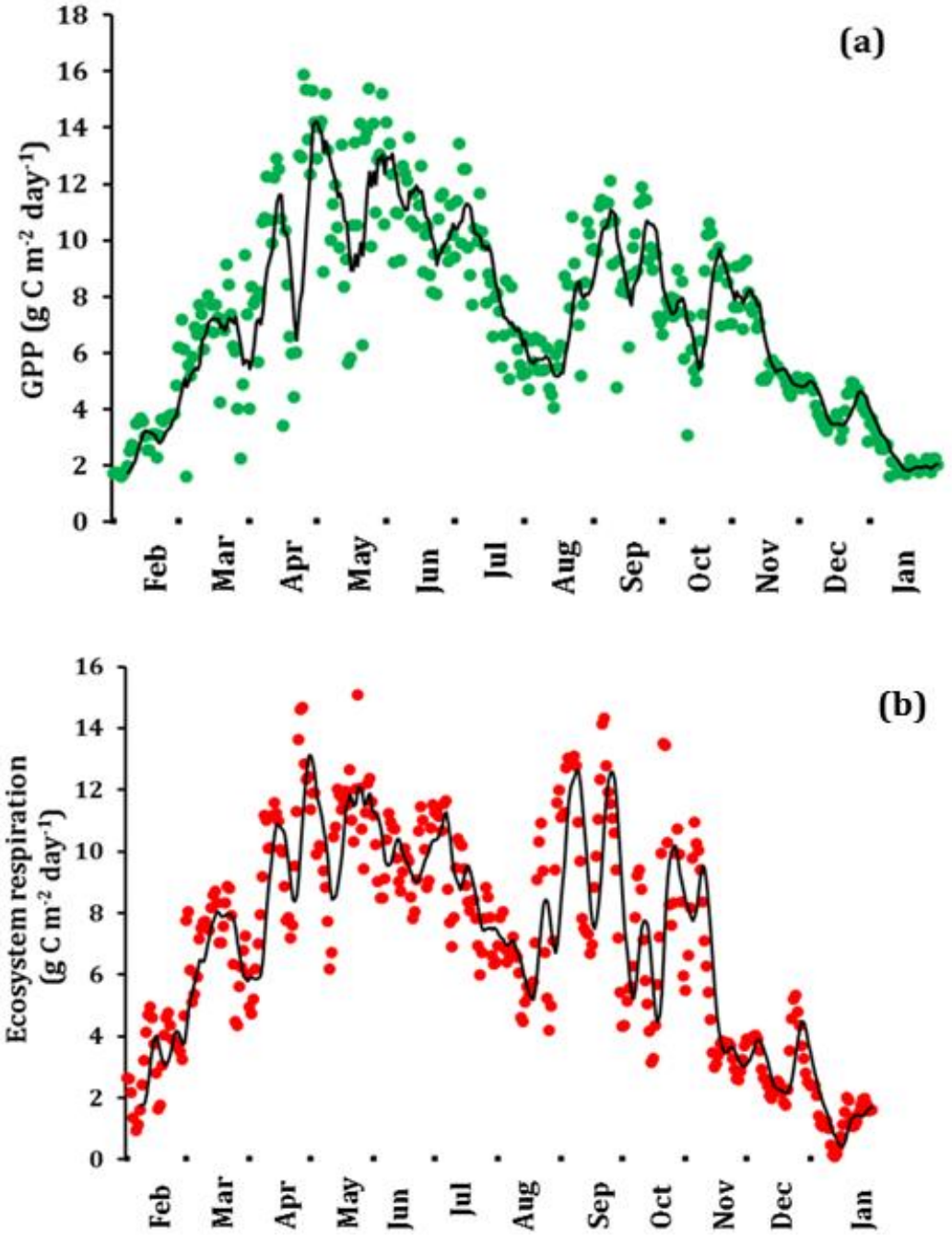

Figure 4.3.1: Daily average of (a) GPP (Gross primary productivity); (b) Ecosystem respiration (Re); daily average in figures are indicate by dots and bold lines indicate 7 days moving average.

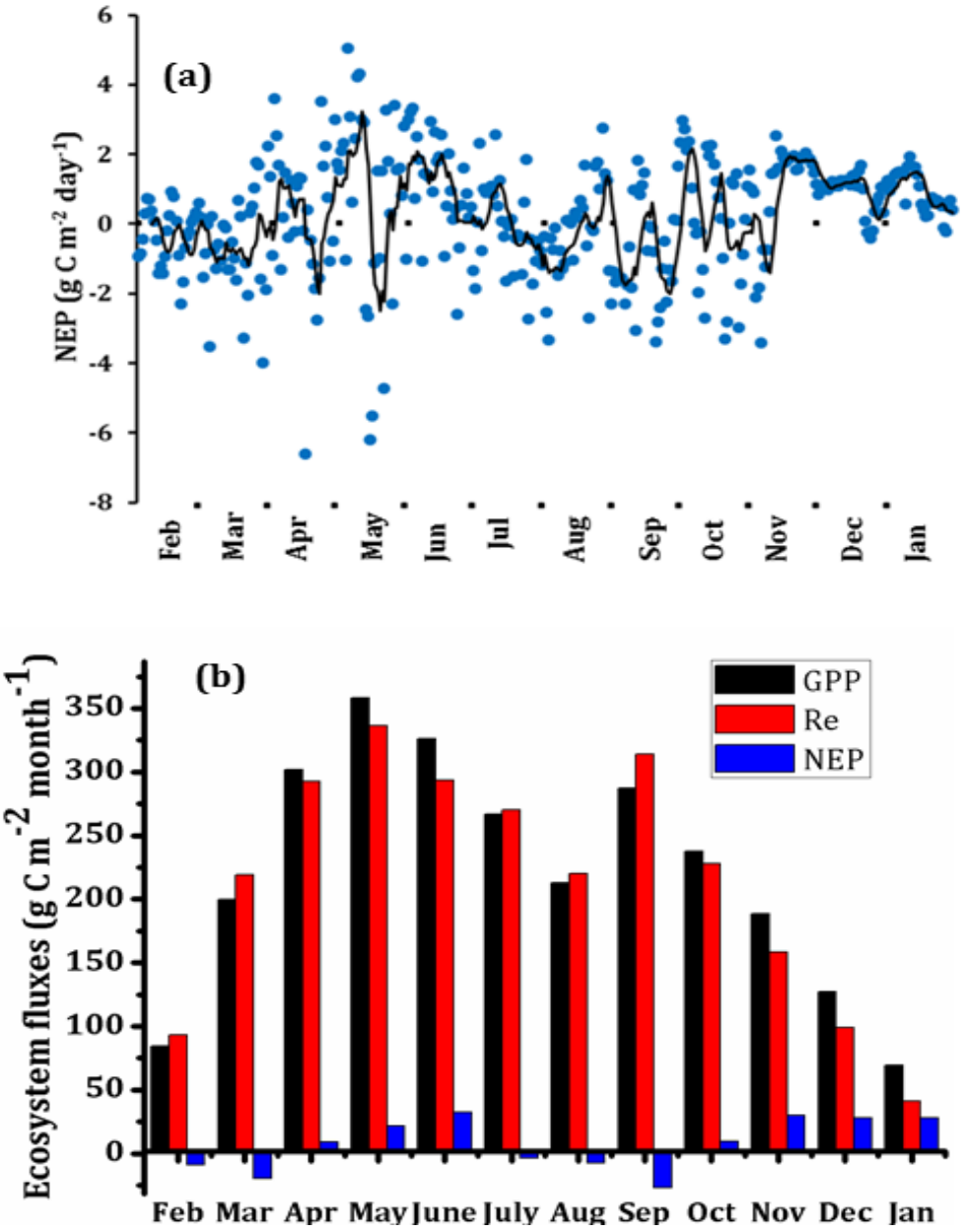

Figure 4.3.2: (a) Daily averages of NEP (net ecosystem productivity), daily averages in figures are indicated by dots and bold line indicates 7 days moving average.

(b) Monthly total of gross primary productivity (GPP), ecosystem respiration (Re) and net ecosystem productivity (NEP).

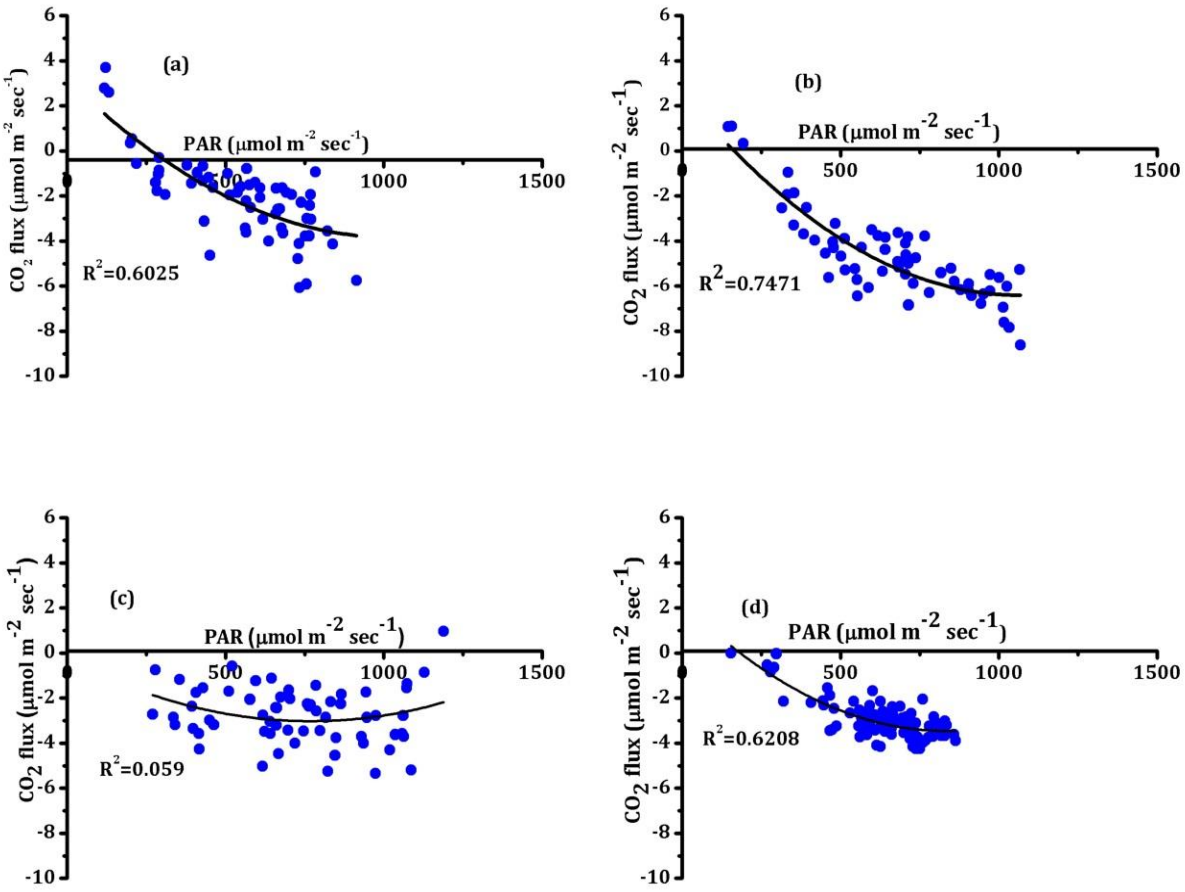

Figure 4.3.3: Relationship between day time average of PAR and CO_2 flux during different months of study (a) March –April 2016; (b) May –June 2016; (c) July, 2016-August, 2016; (d) September-November 2016.

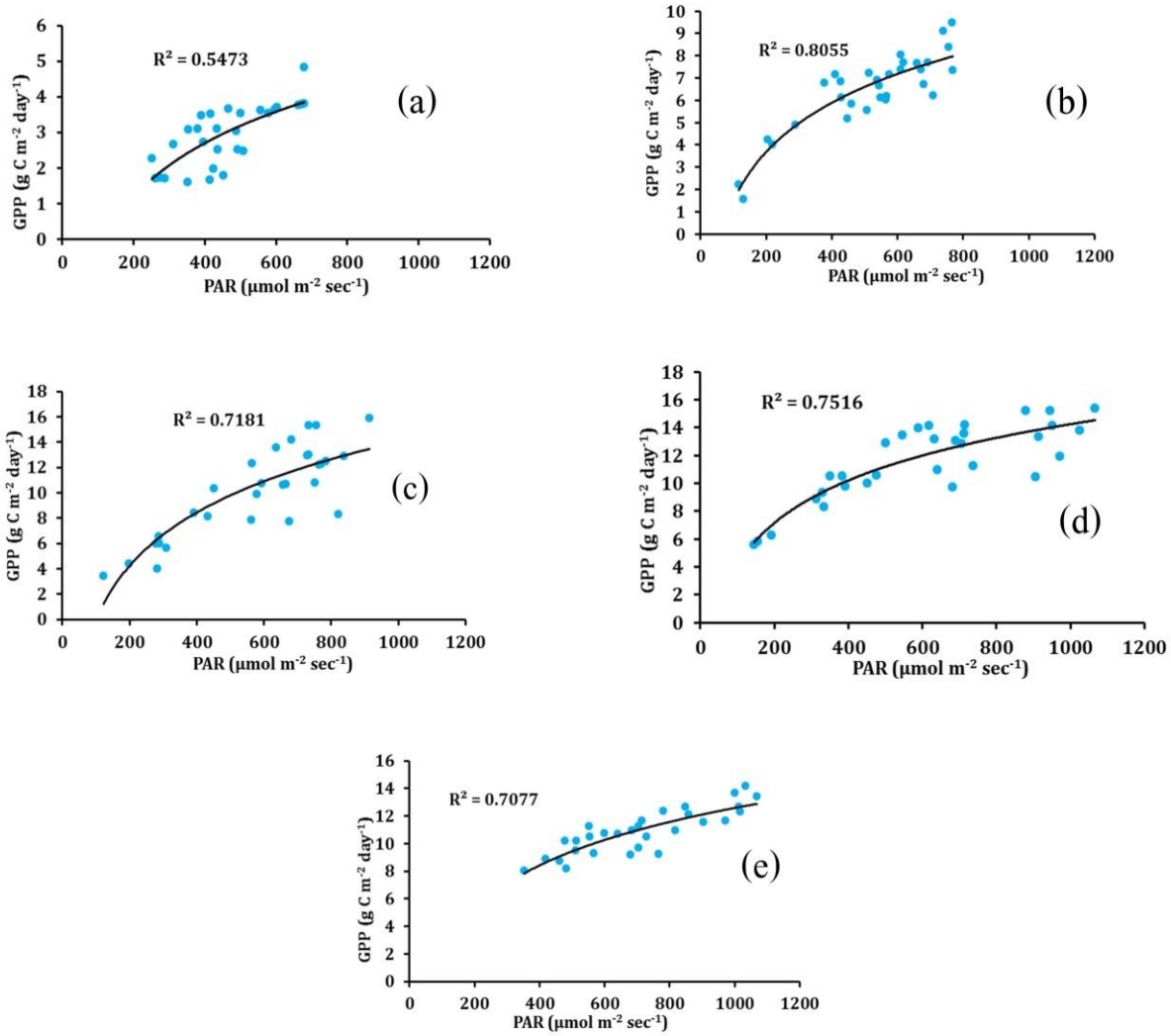

Figure 4.3.4: Relationship between daily averaged GPP and PAR (Photosynthetically active radiation) during different months, (a) February (b) March (c) April (d) May (e) June.

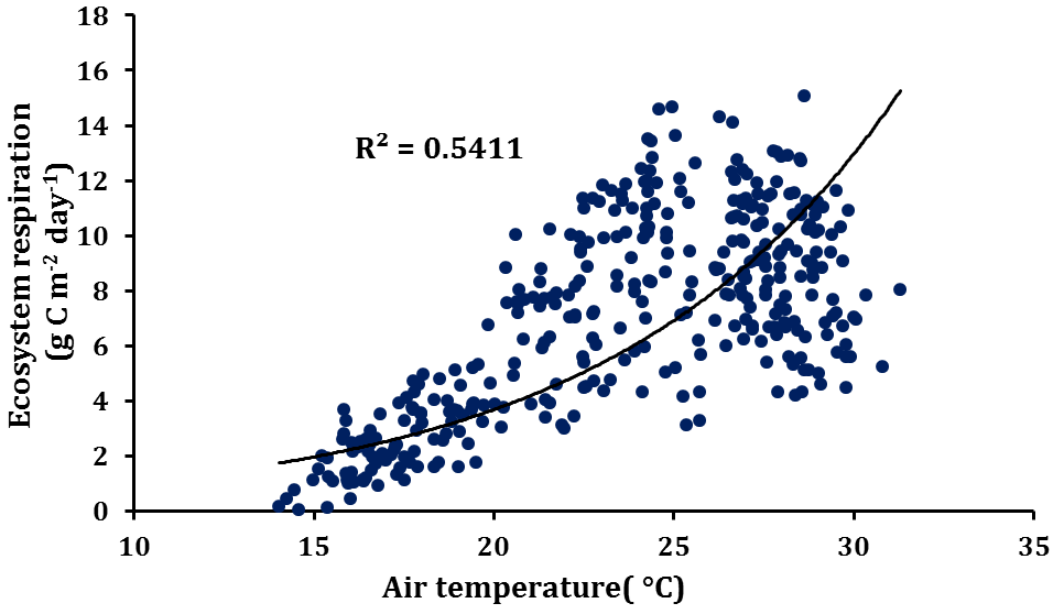

Figure 4.3.5: Relationship between daily average of air temperature and ecosystem respiration (Re) for the whole period of study.

4.4 . Seasonal variations of different soil parameters and their relationship with ecosystem respiration:

4.4.1. Soil physicochemical parameters:

The soil of the forest ecosystem under study is characterized as silty sand in texture (93.5 % sand, 5.5 % silt, clay 1.1%) with average pH of 5.74 ±0.24 . Electrical conductivity of 22 µ S cm^{-1} and 15.63 µ S cm^{-1} were recorded in upper depth and lower depth of soil respectively. The average porosity and water holding capacity of the site were 52.48 and 49.24 % respectively. The mean available nitrogen recorded in the soil was 281±0.3 Kg ha^{-1}, phosphorous 19.2 ± 0.43 kg $ha^{-1}$and potassium 170 ± 0.29 Kg ha^{-1}.

4.4.2. Soil organic carbon (SOC) in %:

The range of organic carbon estimated from soil samples collected from four different sites around the tower during four different seasons (table 4.4.1-4.4.4) were between 1.31% to 1.71% in the upper layer(0-15 cm) whereas it lies between 0.31%- 0.79% in the lower depth (15-30 cm). Seasonal average of SOC (fig 4.4.1) in upper depth depicted highest value of 1.67 % in winter and lowest of 1.4 % in pre-monsoon. The average SOC content of 1.47 and 1.56 % was estimated in upper depth of soil collected during monsoon and post monsoon season. In the samples collected from lower depth, highest

SOC of 0.74% and lowest value of 0.35 % was estimated in winter and pre monsoon seasons respectively. The calculated SOC in monsoon and post monsoon soil samples of lower depth were 0.36 % and 0.54 % respectively.

4.4.3. Soil bulk density (Mg m^{-3}):

Results of bulk density of forest soil are presented in table 4.4.5- 4.4.8, the samples were collected from four sites around the flux tower in four different seasons (winter, pre-monsoon, monsoon and post monsoon). Results presented in the table 4.4.5-4.4.8 are from two different depths 0-15 cm and 15-30 cm. In upper depth the calculated BD was found between 0.86 Mg m^{-3} and 1.26 Mg m^{-3} and in lower depth the range of BD recorded was in between 0.99 Mg m^{-3} and 1.35 Mg m^{-3}. The results of seasonal variation (average) of BD in the upper depth depicted maximum BD of 1.2 Mg m^{-3} in the monsoon season (fig 4.4.2) and minimum BD of 0.91 Mg m^{-3} in the winter season. Similar seasonal trend was also observed in the lower depth with maximum BD of 1.31 Mg m^{-3} in monsoon and minimum of 1.07 Mg m^{-3} in the winter.

4.4.4. Soil temperature (°C):

Diurnal variations (monthly average) of soil temperature at three different depths (5 cm, 15 cm and 40 cm) during four seasons of study are presented in figure 4.4.4. Similar pattern of variation was observed in all the three depths. Diurnal average of soil temperature ranged between 16.33 °C and 29.03 °C throughout the period of study. Out of the three depths of measurement the minimum temperature 16.33°C during winter season and maximum 29.03 °C during monsoon were recorded at 5 cm depth.

4.4.5. Ecosystem respiration (g C m^{-2} $month^{-1}$):

Seasonal average of ecosystem respiration was computed from the monthly total ecosystem respiration (fig 4.4.6). Computed seasonal average indicated peak respiration of 282.83 g C m^{-2} $month^{-1}$ in pre-monsoon season and minimum of 77.99 g C m^{-2} $month^{-1}$ in winter season. The estimated average of ecosystem respiration in monsoon and post monsoon seasons are 274.50 g C m^{-2} $month^{-1}$ and 193.33 g C m^{-2} $month^{-1}$ respectively.

4.4.6. Soil nitrogen (Kg ha^{-1}):

The mean available nitrogen recorded in upper depth (0-15 cm) and lower depth (15-30 cm) of the soil was 281±0.3 Kg ha^{-1} and 277±0.2 Kg ha^{-1} respectively.

4.4.7. C/N ratio of soil:

Seasonal variations of carbon to nitrogen ratio (C/N) in two different depths are depicted in figure 4.4.10. In the upper soil layer peak average C/N ratio of 4.91 was recorded

during winter season followed by C/N ratio of 3.97 in post monsoon season. The calculated average values of C/N ratio in pre-monsoon and monsoon are 2.86 and 2.79 respectively in the upper depth of soil. In the lower soil depth average maximum and minimum C/N ratio of 1.89 and 1.18 were recorded in winter and monsoon respectively. The calculated values of C/N ratio in the lower depth for pre-monsoon and post monsoon seasons are 1.22 and 1.65 respectively.

4.4.8. Soil organic carbon in terms of mass (Mg C ha^{-1}):

The seasonal mean of SOC concentration in upper depth of soil was converted to mass (figure 4.4.12). In winter 2016, the amount of carbon available in the soil was 22.7955 Mg ha^{-1} which increased slightly to 22.932 Mg ha^{-1} toward the end of study period during post monsoon, 2016. The amount of carbon available in soil in pre-monsoon and monsoon were 24.15 Mg ha^{-1} and 26.46 Mg ha^{-1} respectively.

During the study period from winter season of 2016 to post monsoon season of 2016 the amount of carbon stored in KNP soil was estimated as:

SOC (post monsoon) – SOC (winter)

=22.932 Mg ha^{-1}-22.7955 Mg ha^{-1}

=0.137 Mg C ha^{-1} yr^{-1}

On annual basis amount of carbon stored in the soil was estimated as 0.137 Mg C ha^{-1} yr^{-1} which indicates the potential sink strength of the KNP soil.

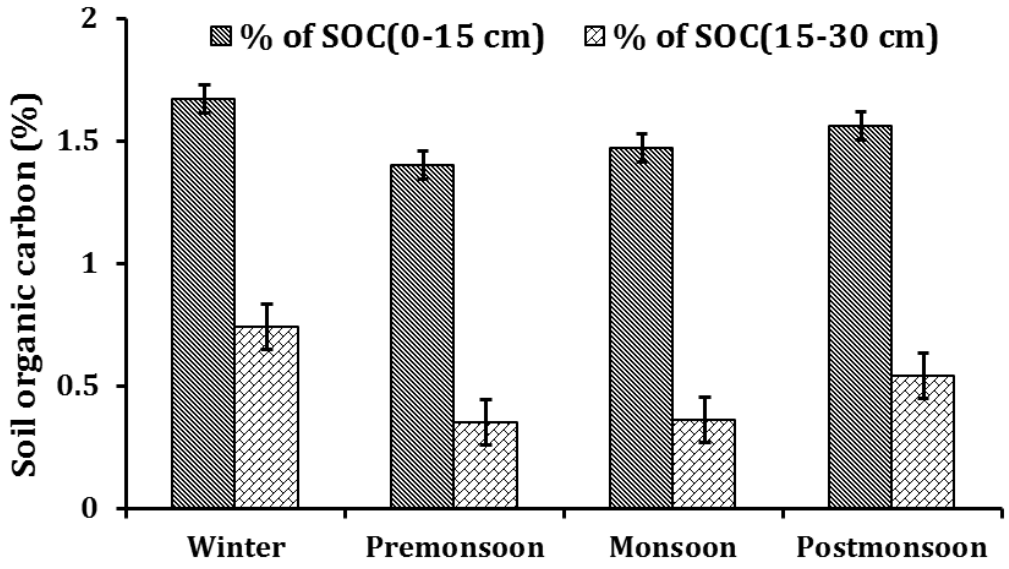

Figure 4.4.1: Seasonal variation of soil organic carbon (SOC).

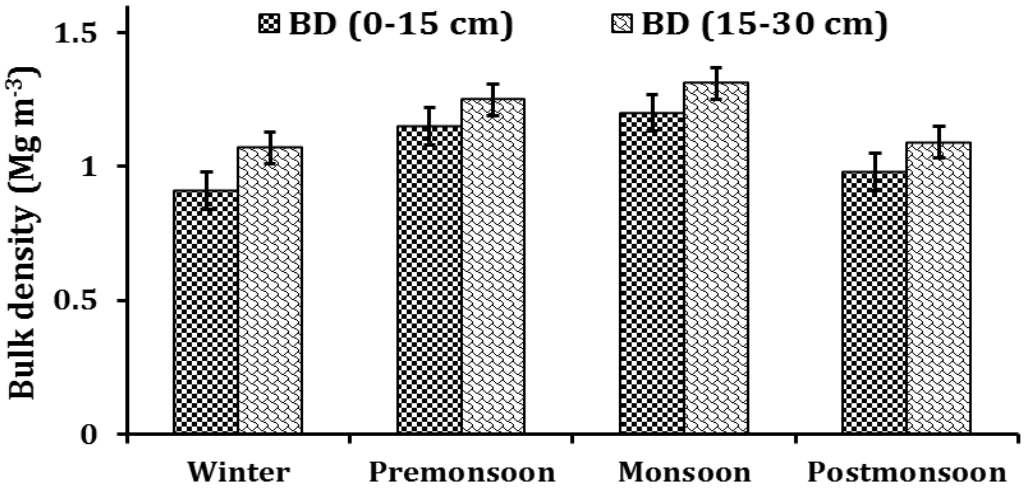

Figure 4.4.2: Seasonal variation of soil bulk density.

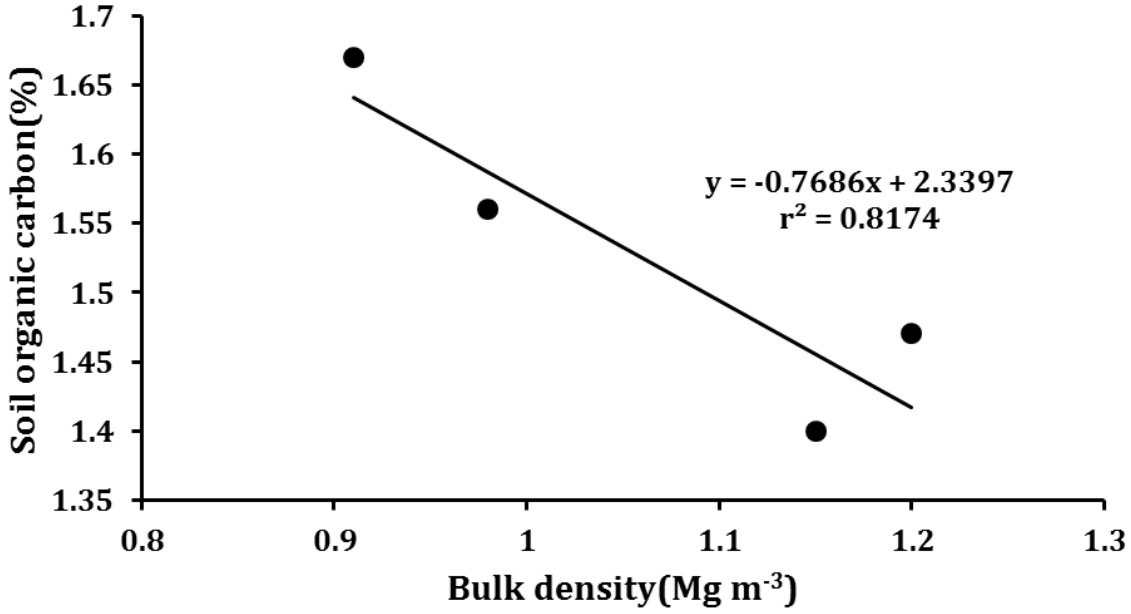

Figure 4.4.3: Relationship between seasonal average of bulk density and seasonal average of soil organic carbon. (adj r^2=0.73, p=0.09).

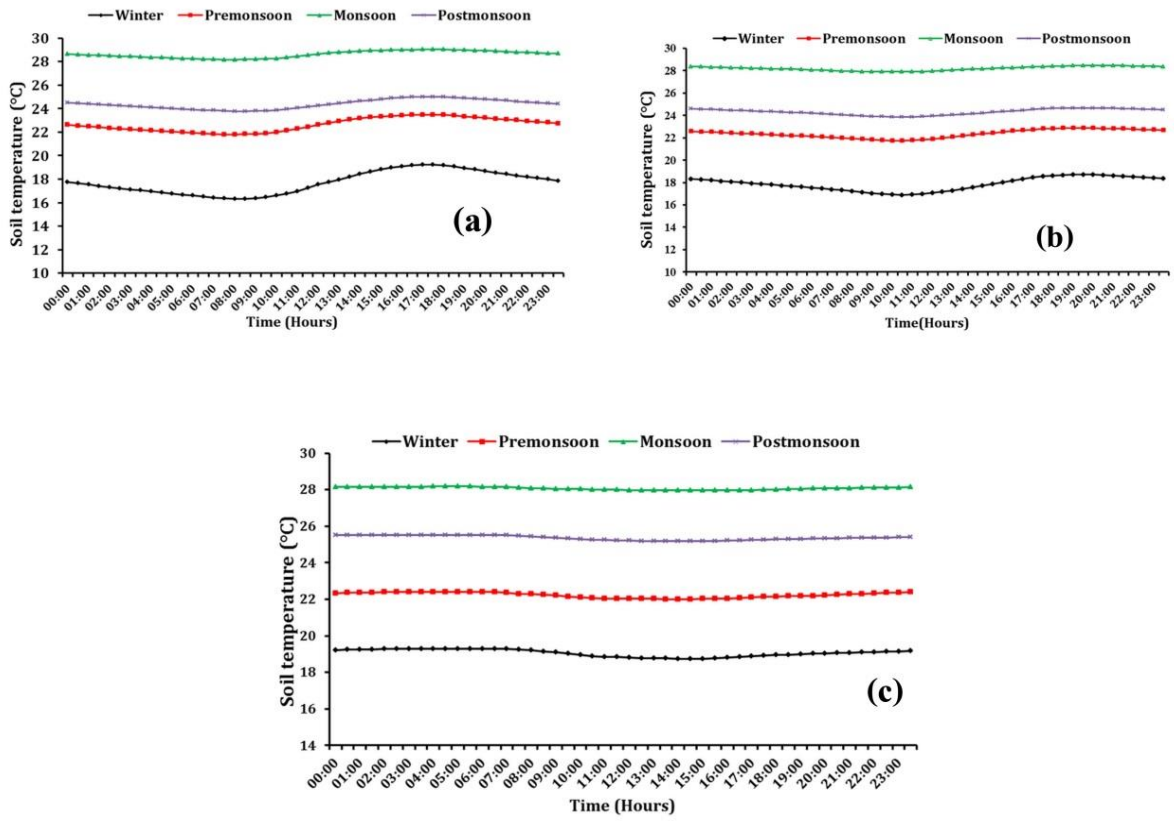

Figure 4.4.4: Variation of soil temperature (°C) at different depths of soil; (a) 5 cm, (b) 15 cm and (c) 40 cm.

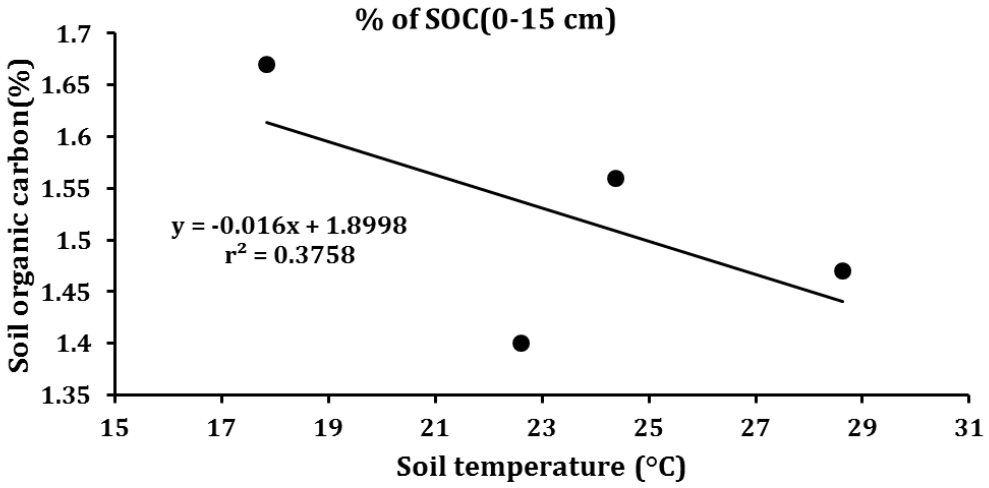

Figure 4.4.5: Relationship between seasonal average of soil temperature and seasonal average of soil organic carbon (adj r^2=0.06, p=0.39).

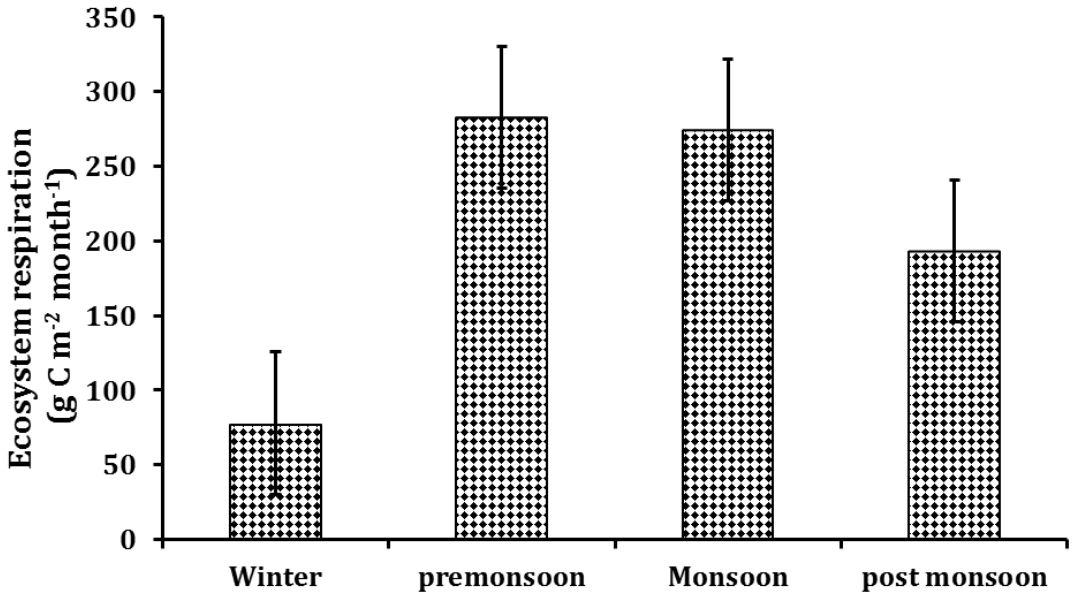

Figure 4.4.6: Seasonal variation in ecosystem respiration (g C m^{-2} $month^{-1}$).

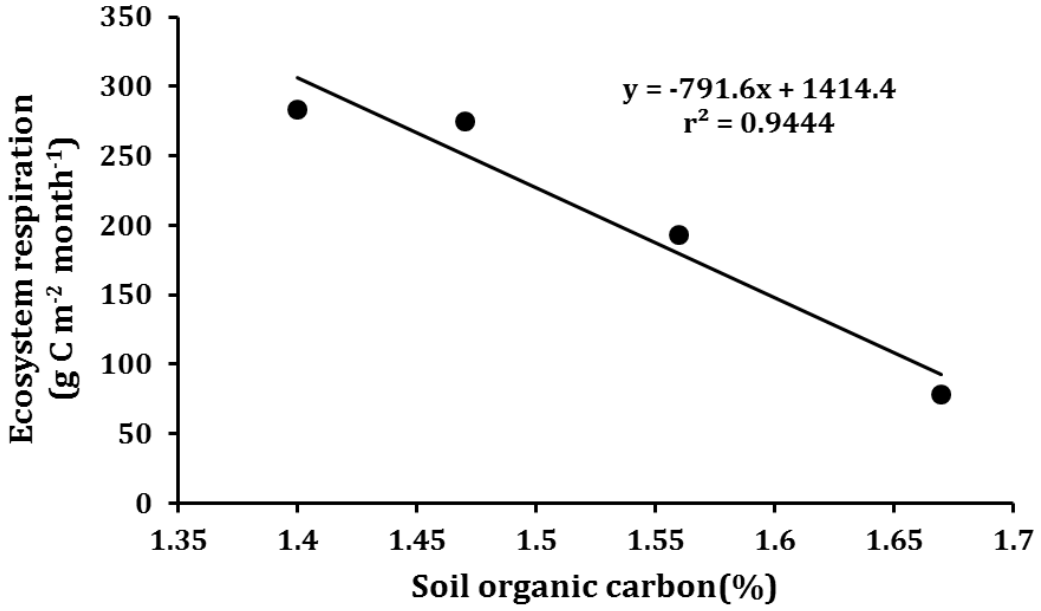

Figure 4.4.7: Relationship between seasonal average of SOC and seasonal average of ecosystem respiration. (adj r^2=0.92, p=0.03).

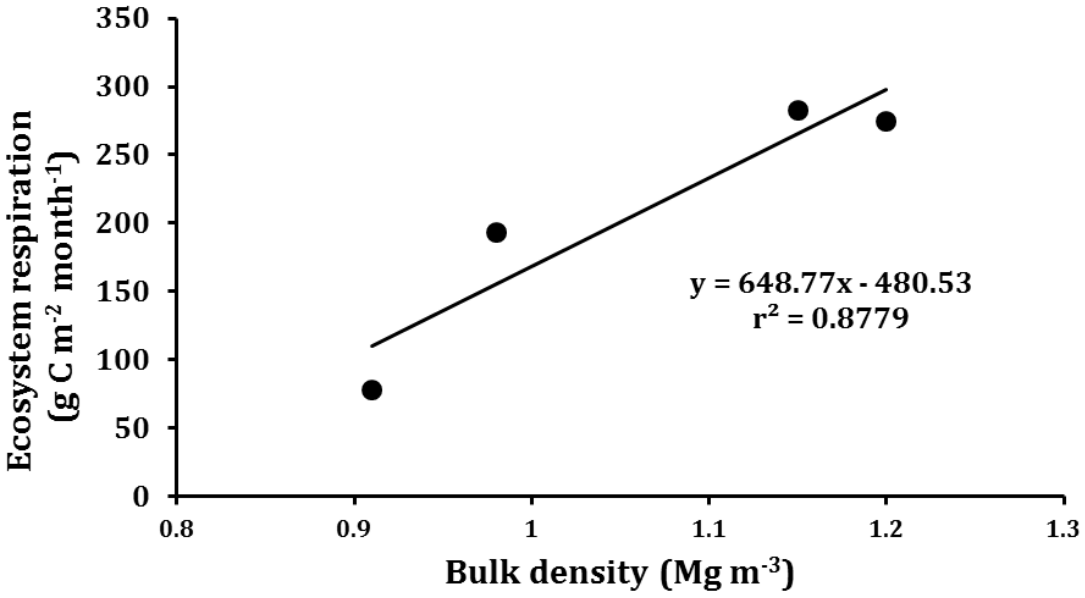

Figure 4.4.8: Seasonal average of soil bulk density vs seasonal average of ecosystem respiration (adj r^2=0.82, p=0.06).

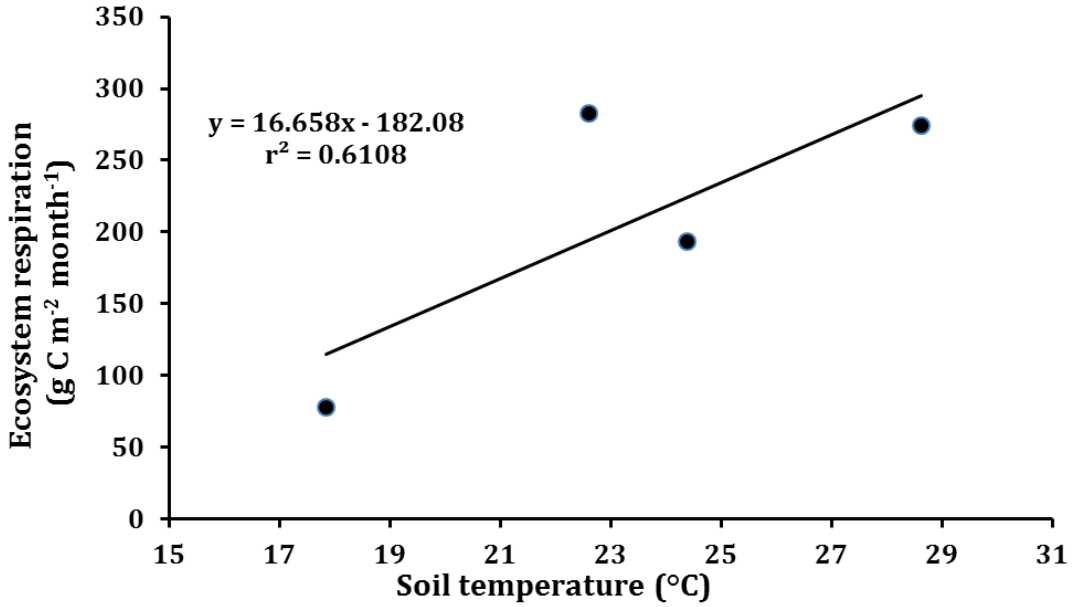

Figure 4.4.9: Relationship between seasonal average of soil temperature and seasonal average of ecosystem respiration (adj r^2=0.42, p=0.22, r^2=0.61).

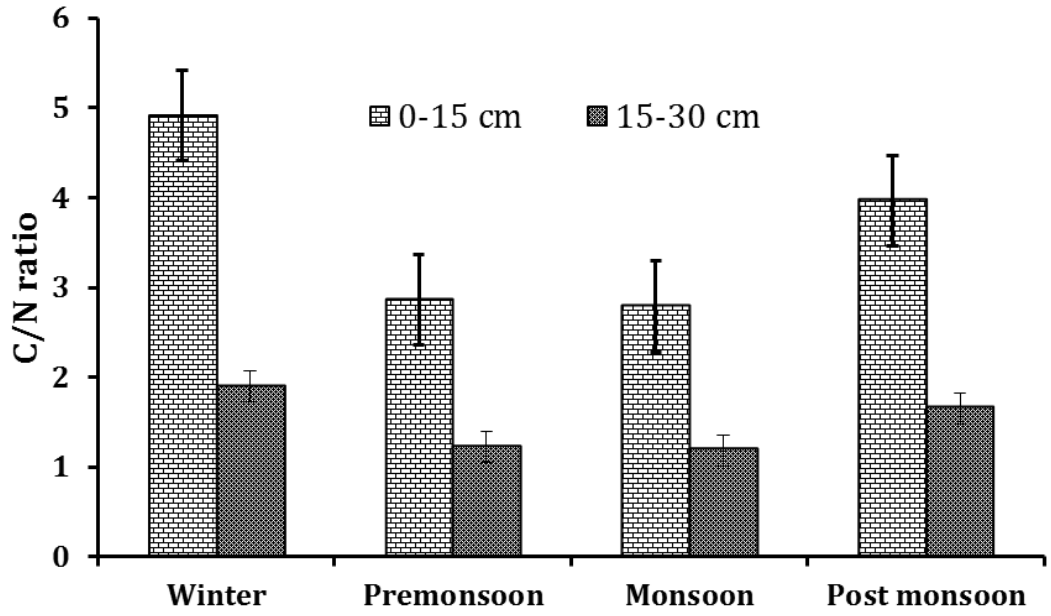

Figure 4.4.10: Seasonal variation of C/N ratio at two different depths of soil.

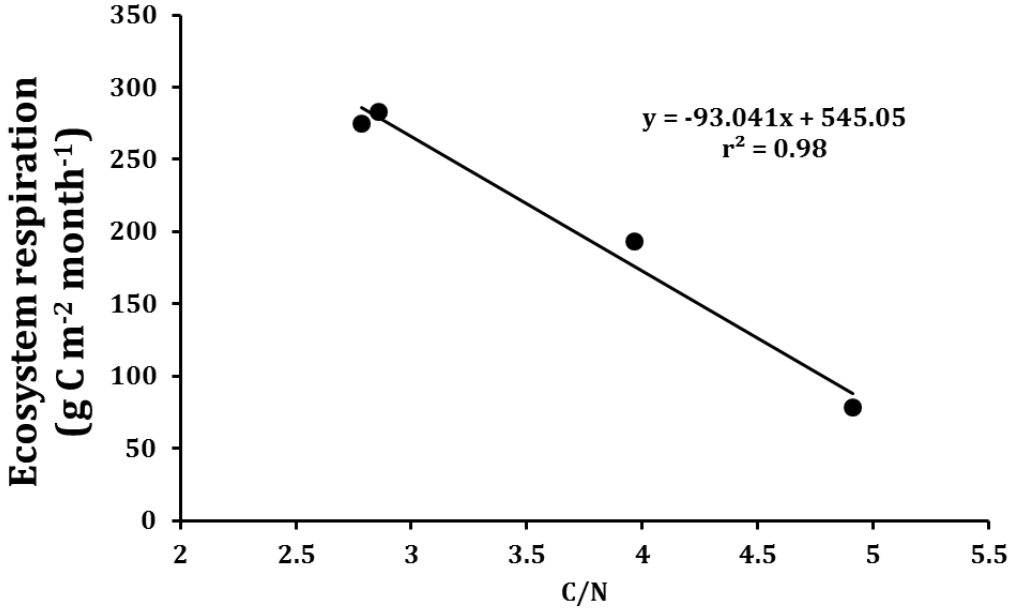

Figure 4.4.11: Impact of C/N ratio (seasonal average) on ecosystem respiration (seasonal average); (adj r^2=0.97, p=0.01).

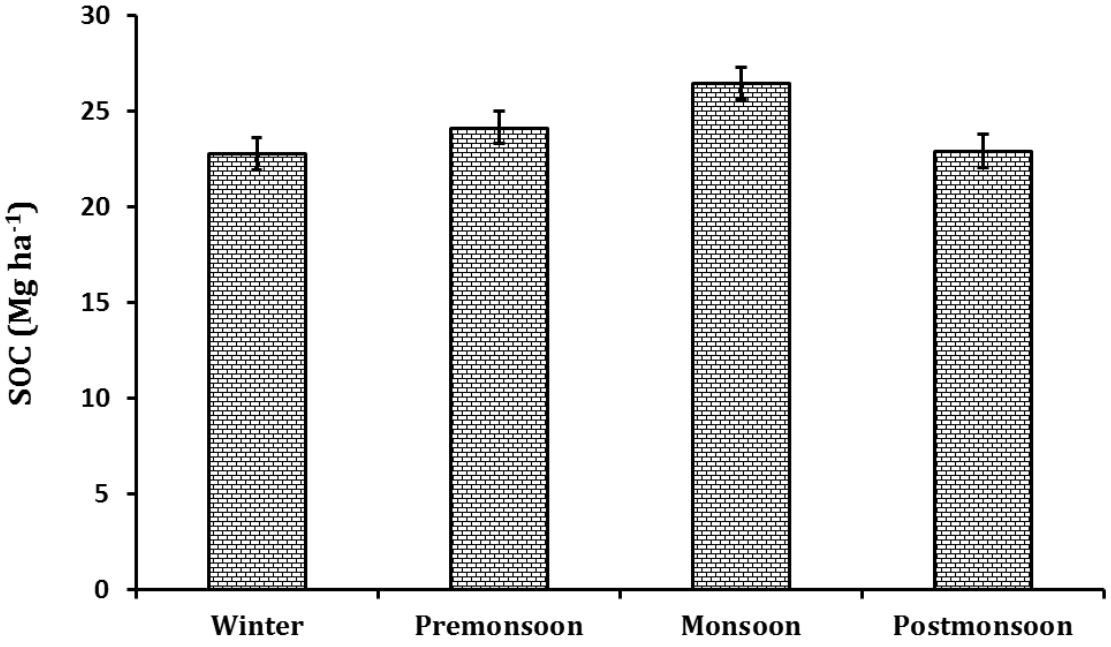

Figure 4.4.12: Seasonal variation in SOC in terms of mass (Mg ha^{-1}) at 0-15 cm depth.

Table 4.4.1: Average SOC (%) of soil samples collected during winter season (±SE) of 2016.

	0-15 cm(average=1.67)	**15-30 cm(average=0.74)**
Site 1	1.66± 0.13	0.79±0.78
Site 2	1.62± 0.22	0.71±0.11
Site 3	1.69± 0.11	0.70±0.26
Site 4	1.71±0.29	0.74±0.33

Table 4.4.2: Average SOC (%) of soil samples collected during pre-monsoon (±SE).

	0-15 cm (average=1.40)	**15-30 cm (average=0.35)**
Site 1	1.31±0.72	0.39±0.27
Site 2	1.42±0.41	0.33±0.38
Site 3	1.49±0.55	0.31±0.16
Site 4	1.39±0.19	0.37±0.44

Table 4.4.3: Average SOC (%) of soil samples collected during monsoon (±SE).

	0-15 cm (average=1.47)	**15-30 cm (average=0.36)**
Site 1	1.42±0.31	0.40±0.61
Site 2	1.47±0.43	0.31±0.36
Site 3	1.50±0.19	0.33±0.55
Site 4	1.49±0.25	0.38±0.29

Table 4.4.4: Average SOC (%) of soil samples collected during post-monsoon (±SE).

	0-15 cm (average=1.56)	**15-30 cm (average=0.54)**
Site 1	1.52±0.18	0.55±0.34
Site 2	1.55±0.12	0.58±0.45
Site 3	1.62±0.23	0.51±0.21
Site 4	1.54±0.35	0.52±0.10

Table 4.4.5: Average BD (Mg m^{-3}) of soil samples collected during winter season (±SE).

	0-15 cm(average=0.91)	**15-30 cm(average=1.07)**
Site 1	0.97±0.17	1.07±0.11
Site 2	0.89±0.32	1.09±0.36
Site 3	0.91±0.19	0.99±0.41
Site 4	0.86±0.28	1.11±0.12

Table 4.4.6: Average BD (Mg m^{-3}) of soil samples collected during pre-monsoon (±SE).

	0-15 cm (average=1.15)	**15-30 cm (average=1.25)**
Site 1	1.11±0.26	1.19±0.39
Site 2	1.20±0.41	1.26±0.26
Site 3	1.12±0.51	1.29±0.31
Site 4	1.18±0.35	1.26±0.70

Table 4.4.7: Average BD (Mg m^{-3}) of soil samples collected during monsoon (±SE).

	0-15 cm (average=1.20)	**15-30 cm (average=1.31)**
Site 1	1.12±0.16	1.31±0.32
Site 2	1.21±0.24	1.29±0.27
Site 3	1.26±0.35	1.35±0.55
Site 4	1.19±0.28	1.30±0.39

Table 4.4.8: Average BD (Mg m^{-3}) of soil samples collected during post-monsoon (±SE).

	0-15 cm (average=0.98)	**15-30 cm (average=1.09)**
Site 1	0.96±0.22	1.01±0.23
Site 2	1.03±0.37	1.11±0.34
Site 3	0.93±0.14	0.99±0.31
Site 4	1.01±0.15	1.23±0.45